Title page

Title:

T6SS contributes to gut microbiome invasion and killing of an herbivorous pest insect by plant-beneficial *Pseudomonas protegens*

Running title:

Role of *P. protegens* T6SS in pest insect invasion

Authors and affiliations:

Jordan Vacheron[1], Maria Péchy-Tarr[1], Silvia Brochet[1], Clara Margot Heiman[1], Marina Stojiljkovic[1], Monika Maurhofer[2#], Christoph Keel[1#]

[1] Department of Fundamental Microbiology, University of Lausanne, Lausanne, Switzerland

[2] Plant Pathology, Institute of Integrative Biology, Swiss Federal Institute of Technology (ETH) Zurich, Zurich, Switzerland

[#]Address correspondence to:

Christoph Keel

Department of Fundamental Microbiology

University of Lausanne

Biophore Building

CH-1015 Lausanne

Switzerland

Phone: +41 21 692 56 36

Fax: +41 21 692 56 05

E-Mail: christoph.keel@unil.ch

Monika Maurhofer

Plant Pathology

Institute of Integrative Biology ETH Zürich

Universitätstrasse 2, CH-8092 Zürich

Switzerland

Phone: +41 44 632 38 69

Fax: +41 44 632 15 72

E-Mail: monika.maurhofer@usys.ethz.ch

Keywords:

Insecticidal bacteria, type VI secretion system (T6SS), *Pseudomonas protegens* CHA0, plant pest insect, *Pieris brassicae*, gut microbiome, *Pseudomonas fluorescens* group

Subject category:

Microbe-microbe and microbe-host interactions

Sources of support (grants/ equipment):

This study was supported by grant 31003A-159520 from the Swiss National Foundation for Scientific Research.

Conflict of interest:

The authors declare no conflict of interest.

Abstract

Pseudomonas protegens are multi-talented plant-colonizing bacteria that suppress plant pathogens and stimulate plant defenses. In addition, they are capable of invading and killing agriculturally important plant pest insects which makes them promising candidates for biocontrol applications. Here we assessed the role of type VI secretion system (T6SS) components of type strain CHA0 during interaction with larvae of the cabbage pest *Pieris brassicae*. We show that the T6SS core apparatus and two VgrG modules, encompassing the respective T6SS spikes (VgrG1a and VgrG1b) and associated effectors (RhsA and Ghh1), contribute significantly to insect pathogenicity of *P. protegens* in oral infection assays, but not when bacteria are injected directly into the hemolymph. Monitoring of the colonization levels of *P. protegens* in the gut, hemolymph and excrements of the insect larvae revealed that the invader relies on T6SS and VgrG1a module function to promote hemocoel invasion. A 16S metagenomic analysis demonstrated that T6SS-supported invasion by *P. protegens* induces significant changes in the insect gut microbiome affecting notably *Enterobacteriaceae*, a dominant group of the commensal gut bacteria. Our study supports the concept that pathogens deploy T6SS-based strategies to disrupt the commensal microbiota in order to promote host colonization and pathogenesis.

Introduction

Bacteria of the *Pseudomonas fluorescens* species complex [1] are commonly associated with plant and soil environments and many exert plant-beneficial functions including the suppression of plant diseases and stimulation of plant defenses [2, 3]. Moreover, a subgroup encompassing the species *Pseudomonas protegens* and *Pseudomonas chlororaphis* is capable of engaging in pathogenic interactions with plant pest insects [4, 5]. The insect-pathogenic and plant-beneficial activities and the capacity to colonize the two contrasting hosts makes these bacteria promising candidates for biocontrol applications in agriculture.

P. protegens type strain CHA0 investigated here is among the best-characterized environmental bacteria with plant-protecting activities [4–7]. CHA0 exhibits potent oral insecticidal activity toward herbivorous larvae of several major Lepidopteran pest insects of agricultural crops [4, 5, 8, 9]. A number of virulence factors contributing to insect pathogenicity have been identified in *P. protegens* CHA0 and the closely related strain Pf-5 [10]. They include several toxins (Fit toxin, hydrogen cyanide, cyclic lipopeptides, rhizoxins) and secreted lytic enzymes (chitinase, phospholipase) [5, 8, 11–14]. The infection process starts with the ingestion of *P. protegens* by the larvae feeding on contaminated plant tissues, leading to the establishment of the invader in the intestinal tract [4]. The bacteria then cross the gut epithelial barrier to invade the hemocoel by a yet unknown mechanism. This passage can take place as early as 24 h after oral infection [4, 5, 8]. Owing to a particular O-antigen decoration of the cell surface, *P. protegens* is capable of resisting antimicrobial peptides (cecropins), i.e. central defense molecules of the insect [15]. In the hemolymph, *P. protegens* proliferates and produces specific virulence factors, notably the insecticidal toxin Fit, resulting in septicemia and ultimately death of the insect [8, 13, 16].

During the establishment in the insect gut and the preparation of the passage through the gut epithelial barrier, invading *P. protegens* cells face competition from the resident gut microbiota. Nothing is currently known about the factors that help the bacteria to be competitive during this crucial infection step. We speculated that type VI secretion system (T6SS)-mediated antagonism toward

commensal gut bacteria might be involved. The T6SS is as a sophisticated nano-weapon used by many Gram-negative bacteria to inject toxic effector proteins into prokaryotic or eukaryotic cells, thereby promoting interbacterial antagonism and virulence in various host environments such as the gut [17–21]. T6SS-mediated strategies are known to help pathogenic bacteria achieve optimal host colonization by displacing host commensal bacteria or eliminating bacterial competitors [19]. This is exemplified by the enteropathogens *Vibrio cholerae* and *Salmonella* Typhimurium which were shown to deploy T6SS-based antibacterial activities for the colonization of animal models [22, 23]. Likewise, T6SS-mediated interbacterial competition promotes host plant colonization by phytopathogenic bacteria [24, 25].

The T6SS apparatus shows striking similarity with the injection machinery of bacteriophages [26, 27] and consists of a membrane-anchoring complex that stands on a baseplate-like structure to which is docked a tube that is composed of Hcp proteins [17, 18, 20, 21]. The Hcp tube is fitted in a contractile sheath-like structure and capped with a spike formed by VgrG proteins [17, 18]. PAAR-domain proteins sharpen the VgrG spike and can function as adapters for effector delivery [18, 28–30]. Antibacterial effectors typically have severe lytic and toxic activity targeting essential bacterial structures such as cell walls, cell membranes and nucleic acids [31–33]. Some effectors impact eukaryotic cells by manipulating the cytoskeleton or exerting cytotoxic effects [19]. Cognate immunity proteins protect the producer bacteria from self-destruction [28, 32]. The T6SS can be fitted with different VgrG-PAAR-effector assemblies allowing a modular usage of the injection device to deliver diverse toxic effectors [28–30, 34].

Here, we report on the characterization of the T6SS core apparatus and two VgrG modules with associated effectors of *P. protegens* CHA0 for their role in insect invasion and pathogenesis. Using larvae of the cabbage butterfly *Pieris brassicae* as plant-feeding insect model, we establish that the T6SS and both VgrG modules contribute to insect killing following oral infection. We show that *P. protegens* uses the T6SS and one of the VgrG modules to promote insect gut colonization and competition with commensal gut bacteria. A 16S-metagenomic analysis demonstrates that TSS6-

supported invasion by *P. protegens* induces significant changes in the insect gut microbiome affecting notably *Enterobacteriaceae*, a dominant group of the commensal gut bacteria.

Material and methods

Bacterial strains, culture conditions and *in vitro* competition assays

Bacterial strains and plasmids used in this study are listed in **Tables S1-S2**. Bacterial culture conditions, isolation and identification of commensal insect gut bacteria and interbacterial competition assays are detailed in the Supplementary Information.

T6SS core apparatus and VgrG module loci in the *P. protegens* CHA0 genome

Gene clusters encoding the T6SS core-apparatus and the VgrG1a and VgrG1b modules were localized in the chromosome of *P. protegens* CHA0 by performing BLAST searches on the NCBI website (https://blast.ncbi.nlm.nih.gov/BlastAlign.cgi) and in the Pseudomonas Genome Database [35] focusing on orthologous genes and shared synteny in *Pseudomonas aeruginosa* PAO1. For the identification of the T6SS and the VgrG proteins, we used blastp with a minimum of 70% of amino-acid sequence identity over at least 70% of the total sequence length. We admitted less sequence conservation for the detection of the effectors associated with the VgrG modules. The functions of the identified proteins were predicted using the NCBI Conserved Domain Database Search [36] and InterPro [37] with default parameters and published information about the related proteins in *P. aeruginosa* [34, 38–40].

Creation of deletion mutants of *P. protegens* CHA0

Mutants of strain CHA0 with deletions of gene clusters encoding (i) the T6SS core apparatus (PFLCHA0_RS30085 through PFLCHA0_RS30180), (ii) the VgrG1a module encompassing predicted spike VgrG1a, effector RhsA and immunity protein RhsI (PFLCHA0_RS30185 through PFLCHA0_RS30220), and (iii) the VgrG1b module encompassing predicted spike VgrG1b, effector Ghh1 and immunity protein GhhI (PFLCHA0_RS15145 through PFLCHA0_RS15190) were constructed. In addition, mutants with individual deletions of the effector genes *rhsA* (PFLCHA0_RS30195) and *ghh1* (PFLCHA0_RS31250) and VgrG spike genes *vgrG1a* (PFLCHA0_RS30185) and *vgrG1b*

(PFLCHA0_RS15170) were generated. Mutants (Table S1) were created using the suicide vector pEMG and the I-SceI system [41] adapted to *P. protegens* [16], with plasmids and primers listed in **Tables S2-S3**.

Pieris brassicae pathogenicity assays

The insect pathogenicity of *P. protegens* strains was assessed in oral infection and injection assays with larvae of *Pieris brassicae*. After hatching, larvae were kept on pesticide-free cabbage plants in a Percival PGC-7L2 plant growth chamber at 25°C and 60% relative humidity, with 16 h of light and 8 h of darkness. For the oral infection assay, 18 2nd instar larvae (body length 1.0-1.5 cm) were selected for each testing condition. Larvae were starved the night before infection and placed individually into six-well culture plates. Each larva was fed with a 0.6-g pellet of artificial diet containing horseradish powder as feeding attractant (adapted from [42]). Diet pellets were inoculated with 5 µl of a suspension containing 5.0 x 10^6 washed bacterial cells in sterile 0.9% NaCl solution. Artificial diet with the same volume of NaCl solution was used as negative control. Larvae that did not consume the entire inoculated diet pellet were excluded from the experiment. After 24 h, larvae from each culture plate were transferred to a Petri dish, fed with fresh sterile artificial diet and monitored for survival every 24 h for seven days.

For the injection assay, bacterial suspensions (2.5 µl containing 10^2 washed cells) were injected via the second proleg directly into the hemolymph of 4th instar *P. brassicae* larvae (body length 2.5-3.0 cm). In each experiment, 18 larvae per treatment were injected and incubated in groups of three in Petri dishes in the plant growth chamber. Larval survival was checked hourly starting at 19 h post-injection.

Pieris brassicae colonization assays

For use in the colonization assay with *P. brassicae* larvae, bacterial strains were marked with a constitutively expressed GFP-tag using pBK-miniTn*7-gfp1* [8]. Oral infection was done as described

above, except that 3rd instar larvae (body length 2.0-2.5 cm) and a larger bacterial inoculum (i.e. 10 µl with 1.0 x 10^7 cells per larva) were used. At 24 h following oral infection, each larva was placed on ice, bled by cutting a proleg to collect the hemolymph and then dissected to extract the entire gut. In addition, excrements were instantly collected from corresponding culture plate wells. Hemolymph, gut and excrement samples were placed in tubes containing 900 µl of sterile 0.9% NaCl solution and homogenized. Aliquots of 10 µl of serially diluted samples were spotted on NA containing 10 µg ml^{-1} of gentamycin. CFU counts were determined with a Fusion FX Spectra imaging platform (Vilber-Lourmat®) by checking colonies for fluorescence under blue light (~470 nm) indicative of growth of GFP-tagged strains.

16S rRNA gene sequencing for metagenomic analysis

Third-instar *Pieris* larvae were orally infected with *P. protegens* strains as described above for the colonization assays. For each condition, 40 larvae were infected. At 24 h following oral infection, each larva was surface-disinfested in ethanol and dissected to extract the gut. For each condition, 10 samples each containing pooled guts from four larvae were prepared. Samples were processed by GenoScreen (Lille, France) for DNA extraction, 16S rRNA gene sequencing and metagenome analysis using the Metabiote® pipeline (see Supplementary Information). Following establishment of the abundance matrix, non-infected insect gut samples in which no *Pseudomonas* OTUs were detected were removed from the analysis (**Table S4**). Sequences affiliated to mitochondria and chloroplasts (indicative of insect tissues and ingested plant material) were removed from the sample prior to analysis. The abundance matrix was loaded into Calypso software version 8.18 [43] using total sum scaling (TSS) and cumulative sum scaling (CSS) normalization [44]. Statistical analysis for 16S-metagenomic data (PCAs, calculation of diversity indexes, and comparison of taxa abundances between treatments) were done using Calypso software.

Statistical analysis of data

Data were statistically analyzed using R studio version 3.3.2 (http://www.rstudio.com/) and considered significantly different when $P < 0.05$. For oral pathogenicity assays with *P. brassicae*, only sample sets with less than two dead larvae out of 18 in the non-infected control were considered for statistical analysis. Data were analyzed using the mixed effect Cox model. To identify significant differences between treatments, ANOVA coupled with Tukey's HSD test including Bonferroni correction was employed. For insect colonization and interbacterial competition assays, data were log10-transformed. Student's t-test was performed to detect significant differences between colonization levels of the CHA0 wild type and ΔT6SS mutant. ANOVA followed by Fisher's LSD-test was done to detect significant differences between colonization levels of the CHA0 wild type and ΔVgrG1a-mod and ΔVgrG1b-mod mutants. Data of interbacterial competition assays were analyzed using ANOVA followed by Tukey's HSD test.

Results and discussion

Characterization of gene clusters encoding the T6SS and VgrG modules in *P. protegens* CHA0

To identify T6SS components in *P. protegens* CHA0, we searched for protein homology with the well-annotated T6SS components of *P. aeruginosa* PAO1 [44]. The cluster encoding the unique T6SS core apparatus of CHA0 ranges from *taqQ* (PFLCHA0_RS30085) to *clpV* (PFLCHA0_RS30180) and shows extensive similarity to the H1-T6SS cluster of *P. aeruginosa* PAO1 [39, 46, 47] in terms of sequence identities and synteny (**Fig. 1; Table S5**). A near identical T6SS gene cluster exists also in the related strain *P. protegens* Pf-5 [48, 49]. Within the H1-T6SS locus of CHA0, the *tag* encoded proteins (PFLCHA0_RS30085 through PFLCHA0_RS30115) share at least 55% identity with the PAO1 PpkA-PppA and Tag proteins (**Fig. 1; Table S5**) that are involved in T6SS signaling and regulation [18, 20, 50]. The 13 conserved *tss* genes upstream of the *tag* genes are required for the assembly of the T6SS core components including baseplate, membrane complex, sheath and tube [17, 21, 29, 51, 52].

T6SS-associated membrane-puncturing devices are mainly composed by VgrG proteins forming a spike that is sharpened by associated PAAR proteins [29, 30]. We identified two proteins in CHA0 that share more than 70% identity with the spike proteins VgrG1a (PA0091) and VgrG1b (PA0095) of *P. aeruginosa* PAO1 [34, 38] and to which we attributed the same names (**Fig. 1; Table S5**). Both predicted CHA0 spike proteins harbor a conserved VI_Rhs_Vgr domain (TIGR03361), which identifies them as typical members of the T6SS Vgr protein family [47]. The CHA0 *vgrG1a* gene (PFLCHA0_RS30185) is located adjacent to the T6SS core apparatus genes whereas CHA0 *vgrG1b* (PFLCHA0_RS15170) is located distant from the T6SS locus (**Fig. 1**), however, in notable vicinity of the locus encoding the insecticidal toxin Fit [53].

The *vgrG* genes are often located in clusters with genes encoding toxic T6SS effectors along with adaptor and cognate immunity proteins [29]. We found that *vgrG1a* and *vgrG1b* of CHA0 are part of such clusters that we termed here VgrG modules. The predicted VgrG1a module ranges from locus tags PFLCHA0_RS30185 to PFLCHA0_RS30220 (**Fig. 1**; **Table S5**). Within this module, PFLCHA0_RS30195, encodes a putative effector of the rearrangement hotspot (Rhs) protein family

[54], which shares 29% identity over 74% of the entire protein length with the Rhs protein Tse5/RhsP1 (PA2684) of *P. aeruginosa* [33, 34]. A near-identical Rhs effector (99% identity with PFLCHA0_RS30195) belonging to the DNase enzyme family and termed RhsA (PFL_6096) was recently functionally characterized in *P. protegens* Pf-5 along with its cognate immunity protein RhsI (PFL_6097; 99% identity with PFLCHA0_RS30200) [55]. We adopted the same terminology for CHA0. The central part of RhsA of CHA0 harbors numerous Rhs repeats, which are thought to encapsulate the C-terminal toxic domain of T6SS-delivered Rhs-type effectors [28]. Like other Rhs T6SS effectors, RhsA of CHA0 possesses a typical N-terminal PAAR domain, described to bind and sharpen the VgrG spike to facilitate effector translocation into the targeted cell [18, 30, 54]. Moreover, two loci flanking the *rhsA-rhsI* effector-immunity gene pair of CHA0 (PFLCHA0_RS30190, PFLCHA0_RS30210) encode proteins of the DUF1795 superfamily, recently identified as adaptor proteins required for the secretion of PAAR-domain T6SS effectors [18, 30, 55].

The predicted VgrG1b module of CHA0 comprises PFLCHA0_RS15145 through PFLCHA0_RS15170. Predicted proteins share 35% to 74% identity with those encoded by the *P. aeruginosa* PAO1 *vgrG1b* locus (PA0095 through PA0101) [34] located near the H1-T6SS locus (**Fig. 1**; **Table S5**). Within the CHA0 VgrG1b module, PFLCHA0_RS31250 is predicted to encode a T6SS effector that we named Ghh1. It harbors an N-terminal PAAR-like domain and a C-terminal TOX-GHH2 domain with predicted nuclease activity like the orthologous PA0099-encoded effector Tse7 (48% identity) in *P. aeruginosa* [34, 40]. By analogy, we predict that the gene that follows *ghh1* in CHA0 (PFLCHA0_RS15150) encodes the cognate immunity protein and termed it *ghhI.* PFLCHA0_RS15160, upstream of *ghh1*, encodes a protein of the DUF2169 superfamily, members of which have recently been suggested to serve as adaptors or chaperones aiding binding of PAAR-domain T6SS effectors to the VgrG spike [57].

To summarize, our analysis of the genome of *P. protegens* CHA0 identified gene clusters coding for a single T6SS core apparatus and two distinct VgrG modules that we termed VgrG1a module (with spike VgrG1a and effector RhsA) and VgrG1b module (with spike VgrG1b and effector Ghh1). To assess the involvement of these components in insect pathogenicity, insect colonization and competition with

265 the gut microbiome, we compared the activity of wild type CHA0 with mutants in which we deleted
266 the entire T6SS or VgrG module gene clusters (ΔT6SS, ΔVgrG1a-mod or ΔVgrG1b-mod, respectively) or
267 individual genes encoding the respective VgrG spikes or effectors (Δ*vgrG1a*, Δ*vgrG1b*, Δ*rhsA* or Δ*ghh1*,
268 respectively) (**Table S1**).
269
270 **The T6SS contributes to insect pathogenicity of *P. protegens* following oral infection**
271 To assess the relative contribution of the T6SS and the two VgrG modules to the insect pathogenicity
272 of *P. protegens*, we orally infected larvae of the plant pest insect *Pieris brassicae* with the CHA0 wild
273 type and the various T6SS-related mutants and monitored larval survival for one week. After this
274 period, less than 12% of the larvae infected by the CHA0 wild type had survived, whereas almost 90%
275 of the larvae of the control treatment without bacteria administration were alive and healthy (**Fig. 2a**).
276 Larval mortality was significantly lower when they were fed the ΔT6SS, ΔVgrG1a-mod or ΔVgrG1b-mod
277 mutants. More than 25% of these larvae survived, highlighting that the T6SS and the two VgrG modules
278 are involved in the infection process. This was further supported by our finding that CHA0 mutants
279 with individual deletions of the respective Vgr spike (Δ*vgrG1a*, Δ*vgrG1b*) or effector genes (Δ*rhsA*,
280 Δ*ghh1*) were equally impaired in oral pathogenicity towards the *Pieris* larvae (**Figs. S1**).
281 Our previous studies established hemocoel invasion as a crucial step in insect pathogenesis of *P.*
282 *protegens* CHA0 [4, 13]. The bacterium uses a tight control system to specifically activate the
283 production of the insecticidal toxin Fit in this compartment leading to an acute disease phase and the
284 death of the insect [8, 16]. Other toxic metabolites, notably hydrogen cyanide and the cyclic
285 lipopeptide orfamide, contribute to insect killing during this infection step [11]. To address whether
286 the T6SS and the two VgrG modules play a role in the insect hemolymph, we mimicked a systemic
287 infection by directly injecting cells of the CHA0 wild type or the ΔT6SS, ΔVgrG1a-mod or ΔVgrG1b-mod
288 mutants into the hemolymph of *Pieris* larvae. At 24 h post injection, the percentage of surviving larvae
289 sharply declined for all bacterial strains tested, dropping to levels of less than 20% at 30 h post injection
290 (**Fig. 2b**). No differences were observed between the insecticidal effects of the wild-type and mutant

strains (**Fig. 2b**), indicating that the T6SS and the VgrG modules are not involved in the hemocoel phase of pathogenesis.

These findings support a significant role of the T6SS and the two VgrG modules along with their respective spike and effector proteins in insect pathogenesis of *P. protegens*. To our best knowledge, we provide here the first example for the implication of T6SS components in the pathogenicity of an environmental bacterium in a plant pest oral infection model. During the past years, the involvement of T6SS components in pathogenicity, be it direct by subverting host cellular function or indirect by aiding competitive host colonization, has been documented for a number of human and plant pathogenic bacteria [19, 24, 32, 58]. In several cases, mutants defective for T6SS components were reported to be impaired in persistence and interbacterial competitiveness during host interaction [19]. These reports prompted us to speculate that the T6SS and the VgrG modules might be required for the successful establishment of *P. protegens* in the intestinal tract of the insect and thus in competitive interactions with the commensal microbiota populating this environment.

The T6SS of *P. protegens* contributes to insect invasion

We examined whether the reduced insect pathogenicity of the T6SS and VgrG module deficient mutants of *P. protegens* CHA0 is linked to a reduced capability of insect invasion following oral infection. To address this, we performed *in vivo* colonization assays with GFP-tagged variants of the bacteria and monitored their establishment in the gut, the hemolymph, and the excrements of *P. brassicae* larvae 24 h after oral infection. We deliberately chose this sampling time point because after this incubation period the first larvae started to die (**Fig. 2a**), implying that pseudomonads by then began to breach the gut epithelial barrier to gain the hemolymph, i.e. a crucial step of insect invasion at the onset of systemic infection. Compared with the wild type, the ΔT6SS mutant was only slightly, but significantly, impaired in its capacity to establish in the insect gut (**Fig. 3a**) but was strongly hampered in its capacity to establish in the hemolymph (**Figs. 3b**). Interestingly, only one of the two VgrG modules appeared to be implicated in insect invasion. Indeed, the ΔVgrG1a-mod mutant was

largely unable to cross the gut epithelial barrier of the *Pieris* larvae to reach the hemolymph whereas the ΔVgrG1b-mod mutant established in this compartment at wild-type levels (**Fig. 3b**). At this time point, both VgrG module mutants were not significantly affected in their gut colonization abilities (**Fig. 3a**). The analysis of the larval excrements indicated that although ingested bacteria established in the insect gut, a significant fraction was cleared from the larvae at roughly the same cell numbers for all strains tested (**Fig. 3c**).

Together these results indicate that the *P. protegens* T6SS has a significant role in gut colonization and preparation of the subsequent passage of the invader into the insect blood system. This is in line with recent reports about the contribution of T6SSs to gut invasion by enteropathogenic *Salmonella, Shigella* and *Vibrio* [22, 23, 59, 60] and to host colonization by various other animal and plant pathogens [19, 24]. Hemolymph invasion by *P. protegens* CHA0 required a functional VgrG1a module. Interestingly, the VgrG1b module had no apparent role in insect colonization although it contributed significantly to insect pathogenicity. This suggests that *P. protegens* employs the two VgrG modules for different activities during pathogenesis of which that of the VgrG1a module is in competitive host colonization (see also following chapter) whereas the exact function of the VgrG1b module needs to be addressed in further studies. Bacteria equipped with T6SSs commonly harbor several VgrG modules along with specific effectors providing them with diverse functionalities during interaction with the host or other bacteria as exemplified by studies on *P. aeruginosa* [34, 45] and enteropathogenic *Escherichia coli* [61].

T6SS-mediated modification of the insect gut microbiome composition by *P. protegens*

Since the T6SS is known to function as major antibacterial weapon in pathogenic and commensal pseudomonads [24, 32, 34, 45, 55], we speculated that a potential role of the T6SS components in insect pathogenesis of *P. protegens* could be to eliminate commensal bacteria within the insect gut thereby facilitating the establishment of the invader in this niche and preparing the access to the gut epithelial barrier for passage into the hemocoel. To test this hypothesis, we performed a 16S RNA gene

343 metagenomic analysis of the gut bacterial microbiota of *P. brassicae* at the larval stage, both in
344 presence and absence of *P. protegens* infection. Gut samples were analyzed after 24 h, i.e. at the same
345 time insect colonization was monitored.

346 We sequenced 50 samples corresponding to five conditions (non-infected control; infection with
347 wild type CHA0 or ΔT6SS, ΔVgrG1a-mod or ΔVgrG1b-mod mutants), with 10 samples per condition and
348 four *Pieris* guts pooled per sample and generated a total of 763,328 high-quality reads. On average,
349 12,722 high-quality filtered reads per sample were obtained. Sequences clustered into 160 different
350 OTUs at a sequence identity cut-off of 97%. Rarefaction curves affirmed that the bacterial diversity in
351 each sample was fully described (**Fig. S2**). The gut bacterial microbiome of healthy insects fed with
352 non-inoculated diet was composed mainly of two bacterial phyla, i.e. Firmicutes (61.7%) and
353 Proteobacteria (38.1%), while other phyla accounted for less than 0.2% of the total abundance (**Fig.**
354 **S3**). The two bacterial families *Enterococcaceae* (58.7%) and *Enterobacteriaceae* (40.4%) were
355 dominant in the gut of the *P. brassicae* larvae (**Fig. 4a**). Other bacterial families constituted less than
356 1% of the total bacterial abundance. More than 99.9% of the sequences affiliated to the
357 *Enterococcaceae* family corresponded to a single OTU (denovo2983) associated with the genus
358 *Enterococcus* (**Table S6**). In the *Enterobacteriaceae* more than 96.1% of the sequences were associated
359 with a single OTU (denovo3889) identified as genus *Enterobacter*. Our analysis provides the first data
360 about the composition of the gut bacterial community of this important Lepidopteran plant pest.
361 Previous studies specified *Enterobacter* sp. as dominant members of the larval gut microbiota of the
362 related insect *Pieris rapae* [62, 63]. *Enterobacter* and *Enterococcus* are commonly found in the gut of
363 Lepidopteran species [64, 65] and can provide beneficial services to their host. For example, they
364 provide enzymatic functions that permit the detoxification of ingested phenolic plant defense
365 compounds [66] or may act as bodyguards against bacterial pathogens invading the insect gut, e.g. by
366 forming a protective biofilm on gut epithelial cells, by producing antimicrobials such as bacteriocins or
367 by inducing insect defenses [67, 68].

We analyzed to what extent invasion by *P. protegens* CHA0 or its T6SS-related mutants shapes the bacterial community in the *P. brassicae* gut. We retrieved a single abundant *Pseudomonas* OTU (denovo2125) from the gut samples *of P. protegens*-treated larvae, which corresponded to the inocula fed to the insects as verified by Blast analysis (100% identity) (**Fig. 4a**). The bacterial alpha diversity was not strongly affected by the presence of CHA0 or the T6SS-related mutants according to the Simpson and Chao indices (**Fig. S4**). The observed significant increase of the diversity at family and genus levels according to the Shannon-Weaver index (Fig. S4a) could be due to the reduction of the most abundant species following *P. protegens* invasion facilitating the detection of other taxa. Moreover, PCA indicated that the beta-diversity remained stable at the phylum and class levels for all tested conditions (**Fig. S5a-5b**). However, at the family and genus levels, the control condition was distant from the other conditions, which reflects the effect of *Pseudomonas* invasion (**Fig. S5c-5d**). The dominance of two bacterial families (*Enterococcaceae*, *Enterobacteriaceae*) in the *P. brassicae* gut made it difficult to observe significant shifts in the remaining fraction of gut bacteria, which accounted for less than 1% of the total bacterial abundance in each condition. Hence, we focused our analysis on the impact of *Pseudomonas* invasion on the relative abundance of *Enterococcaceae* and *Enterobacteriaceae*. Infection by *P. protegens* CHA0 caused a non-significant, mild decrease ($P < 0.09$) in the abundance of *Enterococcaceae*, which did not depend on the bacterial T6SS or VgrG modules (**Fig. 4b**). This finding is not unexpected, since the T6SS is thought to be ineffective against Gram-positive bacteria [32, 69–71]. By contrast, gut invasion by CHA0 resulted in a significant decline of the *Enterobacteriaceae* population in the insect intestines, which required the presence of a functional T6SS (**Fig. 4c**). The two VgrG modules might have contributed to the observed effect to some extent (**Fig. 4c**), however, the high variability among the samples did not allow us to statistically fully affirm this observation.

To confirm the findings of the 16S metagenomic analysis, we isolated bacteria from the gut of *P. brassicae* larvae in order to test them in *in vitro* competition assays against *P. protegens* CHA0 and the T6SS and VgrG module mutants. We repeatedly obtained colonies with two distinct morphologies,

394 which we purified and identified by 16S rRNA gene sequencing exclusively as *Enterococcus* sp. and
395 *Enterobacter* sp., respectively. In confrontation assays against *Enterobacter*, the competitive index for
396 the wild-type CHA0 was significantly higher than that for the ΔT6SS mutant **(Fig. 5a)**. A similar effect
397 was observed in the competition of *Enterobacter* with the ΔVgrG1a-mod mutant, but not with the
398 ΔVgrG1b-mod mutant. This indicates that *P. protegens* uses its T6SS and the VgrG1a-module to
399 outcompete *Enterobacter.* Contrarily, the the T6SS and the VgrG modules did not contribute to the
400 competitive advantage of *P. protegens* CHA0 in confrontations with *Enterococcus* (**Fig. 5b**). These
401 findings are consistent with the T6SS-mediated reduction of *Enterobacteriaceae* by *P. protegens* in the
402 gut microbiome of *Pieris* observed in the 16S-metagenomic analysis (**Fig. 4c**).
403 Collectively, these results demonstrate that during invasion of *P. brassicae* larvae *P. protegens*
404 uses the T6SS to modify the composition of the gut microbiome of the insect, thereby targeting and
405 eliminating in particular bacteria of the genus *Enterobacter* that constitute one of the two dominant
406 groups of commensals present in the intestinal tract of the plant pest. For *Enterobacter* killing, *P.*
407 *protegens* appears to deploy the T6SS primarily with the associated VgrG1a module which is equipped
408 with the DNase effector RhsA. Commensal gut bacteria may form a protective layer at the gut surface,
409 preventing systemic infections by entomopathogens [65, 68]. It is plausible that T6SS-mediated killing
410 of commensal *Enterobacter* by *P. protegens* might locally disrupts this protective layer allowing the
411 invader to reach the hemolymph and kill the insect (**Fig. 6**).
412
413 **Conclusion**
414 The findings of this study support the concept that pathogens deploy T6SS-based strategies to disrupt
415 or otherwise manipulate the commensal microbiota of their host in order to facilitate host colonization
416 as recently demonstrated for the human enteropathogens *Salmonella* Typhimurium [23] and *Vibrio*
417 *cholerae* [72–74]. We provide here the first example of the use of this strategy by an environmental
418 plant-colonizing bacterium to successfully invade a plant pest insect and hence to gain access to an
419 alternative host. We show evidence that the T6SS-mediated changes to the gut microbiome of the pest

insect induced by *P. protegens* are linked to the functional requirement of the T6SS (i) to outcompete specific members of the commensal gut microbiota, (ii) to colonize the insect and ultimately (iii) to promote the pathogenic relationship with the insect host. This is in line with recent work of Fast and colleagues [72] who demonstrated that T6SS activity against commensal gut bacteria supports the pathogenesis of *V. cholerae*. The present work significantly expands our knowledge about the virulence strategies and weaponry that contribute to the capacity of a group of plant-associated pseudomonads to orally infect and kill plant pest insects. Genomic and mutational analyses carried out since the first discovery of the potent insecticidal activity in these pseudomonads [13] so far have identified secreted toxins (Fit toxin, rhizoxins, cyclic lipopeptides, hydrogen cyanide) and lytic enzymes (chitinase, phospholipase) as bacterial determinants promoting insect pathogenesis, i.e. all virulence factors likely deployed by the bacteria to cause direct damage to the insect host at some point during invasion [5, 8, 9, 11, 12, 16]. In turn, the bacteria appear to rely on specific cell surface decorations to escape the insect immune defense [10, 15]. Here, we identified T6SS-mediated manipulation of the gut microbiota as further strategy to promote insect pathogenesis in the repertoire of insecticidal pseudomonads. In our study, *P. protegens* uses the T6SS to target a dominant group of commensals, i.e. *Enterobacter* sp., in the gut of the investigated plant pest. By eliminating part of the population of these commensals, *P. protegens* possibly improves the access to the gut epithelial barrier for the subsequent passage into the hemolymph. Collectively, all these findings advance our understanding of the infection process and allow us to further detail the interaction model between *Pseudomonas* and the insect as illustrated in **Fig. 6**. Since *P. protegens* is also known as an efficient root colonizer and biocontrol agent of crop diseases [4, 6], it will be of interest to study to which extent this bacterium deploys its T6SS weaponry to competitively colonize plants, i.e. its original host.

Acknowledgments

We gratefully acknowledge the group of Philippe Reymond at the Department of Plant Molecular Biology of the University of Lausanne for help with rearing *Pieris brassicae* and with the development

of the artificial diet-based feeding assay. We thank the Biocommunications group (Consuelo De Moraes), Department of Environmental System Science, ETH Zurich for providing eggs of *Pieris brassicae*.

Conflict of interest

The authors declare no conflict of interest.

Supplementary information

Supplementary information is available at The ISME Journal's website.

References

1. Garrido-Sanz D, Arrebola E, Martínez-Granero F, García-Méndez S, Muriel C, Blanco-Romero E, et al. Classification of isolates from the *Pseudomonas fluorescens* complex into phylogenomic groups based in group-specific markers. Front Microbiol. 2017;8:413.

2. Vacheron J, Desbrosses G, Bouffaud M-L, Touraine B, Moënne-Loccoz Y, Muller D, et al. Plant growth-promoting rhizobacteria and root system functioning. Front Plant Sci. 2013;4:356.

3. Mauchline TH, Malone JG. Life in earth - the root microbiome to the rescue? Curr Opin Microbiol. 2017;37:23–28.

4. Kupferschmied P, Maurhofer M, Keel C. Promise for plant pest control: root-associated pseudomonads with insecticidal activities. Front Plant Sci. 2013;4:287

5. Flury P, Aellen N, Ruffner B, Péchy-Tarr M, Fataar S, Metla Z, et al. Insect pathogenicity in plant-beneficial pseudomonads: phylogenetic distribution and comparative genomics. ISME J. 2016;10: 2527–42.

6. Haas D, Défago G. Biological control of soil-borne pathogens by fluorescent pseudomonads. Nat Rev Microbiol. 2005;3:307–19.

7. Haas D, Keel C. Regulation of antibiotic production in root-colonizing *Pseudomonas* spp. and relevance for biological control of plant disease. Annu Rev Phytopathol. 2003;41:117–53.

8. Péchy-Tarr M, Borel N, Kupferschmied P, Turner V, Binggeli O, Radovanovic D, et al. Control and host-dependent activation of insect toxin expression in a root-associated biocontrol pseudomonad. Environ Microbiol. 2013;15:736-50.

9. Ruffner B, Péchy-Tarr M, Ryffel F, Hoegger P, Obrist C, Rindlisbacher A, et al. Oral insecticidal activity of plant-associated pseudomonads. Environ Microbiol. 2013;15:751–63.

10. Keel C. A look into the toolbox of multi-talents: insect pathogenicity determinants of plant-beneficial pseudomonads. Environ Microbiol. 2016;18:3207–9.

11. Flury P, Vesga P, Péchy-Tarr M, Aellen N, Dennert F, Hofer N, et al. Antimicrobial and insecticidal: cyclic lipopeptides and hydrogen cyanide produced by plant-beneficial *Pseudomonas* strains CHA0, CMR12a, and PCL1391 contribute to insect killing. Front Microbiol. 2017;8:100.

12. Loper JE, Henkels MD, Rangel LI, Olcott MH, Walker FL, Bond KL, et al. Rhizoxin analogs, orfamide A and chitinase production contribute to the toxicity of *Pseudomonas protegens* strain Pf-5 to *Drosophila melanogaster*. Environ Microbiol. 2016;18:3509–21.

13. Péchy-Tarr M, Bruck DJ, Maurhofer M, Fischer E, Vogne C, Henkels MD, et al. Molecular analysis of a novel gene cluster encoding an insect toxin in plant-associated strains of *Pseudomonas fluorescens*. Environ Microbiol. 2008;10:2368–86.

14. Rangel LI, Henkels MD, Shaffer BT, Walker FL, Davis EW, Stockwell VO, et al. Characterization of toxin complex gene clusters and insect toxicity of bacteria representing four subgroups of *Pseudomonas fluorescens*. PLOS One. 2016;11:e0161120.

15. Kupferschmied P, Chai T, Flury P, Blom J, Smits THM, Maurhofer M, et al. Specific surface glycan decorations enable antimicrobial peptide resistance in plant-beneficial pseudomonads with insect-pathogenic properties. Environ Microbiol. 2016;18:4265–81.

16. Kupferschmied P, Péchy-Tarr M, Imperiali N, Maurhofer M, Keel C. Domain shuffling in a sensor protein contributed to the evolution of insect pathogenicity in plant-beneficial *Pseudomonas protegens*. PLoS Pathog. 2014; 10:e1003964.

17. Basler M. Type VI secretion system: secretion by a contractile nanomachine. Philos Trans R Soc Lond, B, Biol Sci. 2015; 370. pii20150021.

18. Cianfanelli FR, Monlezun L, Coulthurst SJ. Aim, load, fire: The type VI secretion system, a bacterial nanoweapon. Trends Microbiol. 2016;24:51–62.

19. Hachani A, Wood TE, Filloux A. Type VI secretion and anti-host effectors. Curr Opin Microbiol. 2016;29:81–93.

20. Ho BT, Dong TG, Mekalanos JJ. A view to a kill: the bacterial type VI secretion system. Cell Host Microbe. 2014;15:9–21.

21. Nguyen VS, Douzi B, Durand E, Roussel A, Cascales E, Cambillau C. Towards a complete structural deciphering of type VI secretion system. Curr Opin Struct Biol. 2018;49:77–84.

22. Fu Y, Waldor MK, Mekalanos JJ. Tn-Seq analysis of *Vibrio cholerae* intestinal colonization reveals a role for T6SS-mediated antibacterial activity in the host. Cell Host Microbe. 2013;14:652–63.

23. Sana TG, Flaugnatti N, Lugo KA, Lam LH, Jacobson A, Baylot V, et al. *Salmonella typhimurium* utilizes a T6SS-mediated antibacterial weapon to establish in the host gut. Proc Natl Acad Sci USA. 2016; 113:E5044-51.

24. Bernal P, Llamas MA, Filloux A. Type VI secretion systems in plant-associated bacteria. Environ Microbiol. 2018;20:1–15.

25. Ma L-S, Hachani A, Lin J-S, Filloux A, Lai E-M. *Agrobacterium tumefaciens* deploys a superfamily of type VI secretion DNase effectors as weapons for interbacterial competition *in planta*. Cell Host Microbe. 2014; 16: 94–104.

26. Filloux A, Freemont P. Structural biology: Baseplates in contractile machines. Nat Microbiol 2016; 1: 16104.

27. Silverman JM, Brunet YR, Cascales E, Mougous JD. Structure and regulation of the type VI secretion system. Annu Rev Microbiol. 2012;66:453–72.

28. Alcoforado Diniz J, Liu Y-C, Coulthurst SJ. Molecular weaponry: diverse effectors delivered by the type VI secretion system. Cell Microbiol. 2015;17:1742–51.

29. Cianfanelli FR, Alcoforado Diniz J, Guo M, De Cesare V, Trost M, Coulthurst SJ. VgrG and PAAR proteins define distinct versions of a functional type VI secretion system. PLoS Pathog. 2016;12: e1005735.

30. Shneider MM, Buth SA, Ho BT, Basler M, Mekalanos JJ, Leiman PG. PAAR-repeat proteins sharpen and diversify the type VI secretion system spike. Nature. 2013;500:350–53.

31. Durand E, Cambillau C, Cascales E, Journet L. VgrG, Tae, Tle, and beyond: the versatile arsenal of type VI secretion effectors. Trends Microbiol. 2014;22:498–507.

32. Russell AB, Peterson SB, Mougous JD. Type VI secretion system effectors: poisons with a purpose. Nat Rev Microbiol. 2014;12:137–48.

33. Whitney JC, Beck CM, Goo YA, Russell AB, Harding B, De Leon JA, et al. Genetically distinct pathways

guide effector export through the type VI secretion system. Mol Microbiol. 2014;92:529–42.

34. Hachani A, Allsopp LP, Oduko Y, Filloux A. The VgrG proteins are 'à la carte' delivery systems for bacterial type VI effectors. J Biol Chem. 2014;289:17872–84.

35. Winsor GL, Griffiths EJ, Lo R, Dhillon BK, Shay JA, Brinkman FSL. Enhanced annotations and features for comparing thousands of *Pseudomonas* genomes in the *Pseudomonas* genome database. Nucleic Acids Res. 2016;44:D646-53.

36. Marchler-Bauer A, Bo Y, Han L, He J, Lanczycki CJ, Lu S, et al. CDD/SPARCLE: functional classification of proteins via subfamily domain architectures. Nucleic Acids Res. 2017;45:D200–D203.

37. Finn RD, Attwood TK, Babbitt PC, Bateman A, Bork P, Bridge AJ, et al. InterPro in 2017—beyond protein family and domain annotations. Nucleic Acids Res. 2017;45:D190–D199.

38. Hachani A, Lossi NS, Hamilton A, Jones C, Bleves S, Albesa-Jové D, et al. Type VI secretion system in *Pseudomonas aeruginosa* secretion and multimerization of VgrG proteins. J Biol Chem. 2011;286:12317–27.

39. Hood RD, Singh P, Hsu F, Güvener T, Carl MA, Trinidad RRS, et al. A type VI secretion system of *Pseudomonas aeruginosa* targets a toxin to bacteria. Cell Host Microbe. 2010;7:25–37.

40. Pissaridou P, Allsopp LP, Wettstadt S, Howard SA, Mavridou DAI, Filloux A. The Pseudomonas aeruginosa T6SS-VgrG1b spike is topped by a PAAR protein eliciting DNA damage to bacterial competitors. *PNAS* 2018; **115**: 12519–12524.

41. Martínez-García E, de Lorenzo V. Engineering multiple genomic deletions in Gram-negative bacteria: analysis of the multi-resistant antibiotic profile of *Pseudomonas putida* KT2440. Environ Microbiol. 2011;13:2702–16.

42. David WAL, Gardiner BOC. Rearing *Pieris brassicae* L. larvae on a semi-synthetic diet. Nature 1965; 207: 882–883.

43. Zakrzewski M, Proietti C, Ellis JJ, Hasan S, Brion M-J, Berger B, et al. Calypso: a user-friendly web-server for mining and visualizing microbiome–environment interactions. Bioinformatics. 2017;33:782–3.

44. Paulson JN, Stine OC, Bravo HC, Pop M. Robust methods for differential abundance analysis in marker gene surveys. Nat Methods. 2013; 10:1200–2.

45. Sana TG, Berni B, Bleves S. The T6SSs of *Pseudomonas aeruginosa* strain PAO1 and their effectors: beyond bacterial-cell targeting. Front Cell Infect Microbiol. 2016;6:61.

46. Filloux A, Hachani A, Bleves S. The bacterial type VI secretion machine: yet another player for protein transport across membranes. Microbiology (Reading, Engl) 2008;154:1570–83.

47. Mougous JD, Cuff ME, Raunser S, Shen A, Zhou M, Gifford CA, et al. A virulence locus of *Pseudomonas aeruginosa* encodes a protein secretion apparatus. Science. 2006; 312:1526–30.

48. Hassan KA, Johnson A, Shaffer BT, Ren Q, Kidarsa TA, Elbourne LDH, et al. Inactivation of the GacA response regulator in *Pseudomonas fluorescens* Pf-5 has far-reaching transcriptomic consequences. Environ Microbiol. 2010;12:899–915.

49. Loper JE, Hassan KA, Mavrodi DV, Davis EW, Lim CK, Shaffer BT, et al. Comparative genomics of plant-associated *Pseudomonas* spp.: insights into diversity and inheritance of traits involved in

574 multitrophic interactions. PLoS Genet. 2012;8:e1002784.

575 50. Basler M, Ho BT, Mekalanos JJ. Tit-for-tat: type VI secretion system counterattack during bacterial
576 cell-cell interactions. Cell. 2013;152:884–94.

577 51. Cascales E, Cambillau C. Structural biology of type VI secretion systems. Philos Trans R Soc Lond B
578 Biol Sci. 2012;367:1102–11.

579 52. Zoued A, Brunet YR, Durand E, Aschtgen M-S, Logger L, Douzi B, et al. Architecture and assembly
580 of the type VI secretion system. Biochim Biophys Acta. 2014;1843:1664–73.

581 53. Ruffner B, Péchy-Tarr M, Höfte M, Bloemberg G, Grunder J, Keel C, et al. Evolutionary patchwork
582 of an insecticidal toxin shared between plant-associated pseudomonads and the insect pathogens
583 *Photorhabdus* and *Xenorhabdus*. BMC Genomics. 2015;16:609.

584 54. Ma J, Pan Z, Huang J, Sun M, Lu C, Yao H. The Hcp proteins fused with diverse extended-toxin
585 domains represent a novel pattern of antibacterial effectors in type VI secretion systems. Virulence.
586 2017;8:1189–1202.

587 55. Tang JY, Bullen NP, Ahmad S, Whitney JC. Diverse NADase effector families mediate interbacterial
588 antagonism *via* the type VI secretion system. J Biol Chem. 2018;293:1504–14.

589 56. Unterweger D, Kostiuk B, Pukatzki S. Adaptor proteins of type VI secretion system effectors. Trends
590 Microbiol. 2017;25:8–10.

591 57. Bondage DD, Lin J-S, Ma L-S, Kuo C-H, Lai E-M. VgrG C terminus confers the type VI effector
592 transport specificity and is required for binding with PAAR and adaptor-effector complex. Proc Natl
593 Acad Sci USA. 2016;113:E3931-40.

594 58. Kapitein N, Mogk A. Deadly syringes: type VI secretion system activities in pathogenicity and
595 interbacterial competition. Curr Opin Microbiol. 2013;16:52–8.

596 59. Anderson MC, Vonaesch P, Saffarian A, Marteyn BS, Sansonetti PJ. *Shigella sonnei* encodes a
597 functional T6SS used for interbacterial competition and niche occupancy. Cell Host Microbe.
598 2017;21:769-776.e3.

599 60. Joshi A, Kostiuk B, Rogers A, Teschler J, Pukatzki S, Yildiz FH. Rules of engagement: The type VI
600 secretion system in *Vibrio cholerae*. Trends Microbiol. 2017;25:267–79.

601 61. Ma J, Sun M, Pan Z, Lu C, Yao H. Diverse toxic effectors are harbored by *vgrG* islands for
602 interbacterial antagonism in type VI secretion system. Biochim Biophys Acta. 2018;1862:1635–43.

603 62. Broderick NA, Robinson CJ, McMahon MD, Holt J, Handelsman J, Raffa KF. Contributions of gut
604 bacteria to *Bacillus thuringiensis*-induced mortality vary across a range of *Lepidoptera*. BMC Biology.
605 2009;7:11.

606 63. Robinson CJ, Schloss P, Ramos Y, Raffa K, Handelsman J. Robustness of the bacterial community in
607 the cabbage white butterfly larval midgut. Microb Ecol. 2010;59:199–211.

608 64. Tang X, Freitak D, Vogel H, Ping L, Shao Y, Cordero EA, et al. Complexity and variability of gut
609 commensal microbiota in polyphagous lepidopteran larvae. PLoS ONE. 2012;7:e36978.

610 65. Paniagua Voirol LR, Frago E, Kaltenpoth M, Hilker M, Fatouros NE. Bacterial symbionts in
611 *Lepidoptera*: their diversity, transmission, and impact on the host. Front Microbiol. 2018;9:556.

612 66. Xia X, Gurr GM, Vasseur L, Zheng D, Zhong H, Qin B, et al. Metagenomic sequencing of diamondback

613 moth gut microbiome unveils key holobiont adaptations for herbivory. Front Microbiol. 2017;8:663.

614 67. Shao Y, Chen B, Sun C, Ishida K, Hertweck C, Boland W. Symbiont-derived antimicrobials contribute
615 to the control of the Lepidopteran gut microbiota. Cell Chem Biol. 2017;24:66–75.

616 68. Engel P, Moran NA. The gut microbiota of insects – diversity in structure and function. FEMS
617 Microbiol Rev. 2013;37:699–735.

618 69. Chou S, Bui NK, Russell AB, Lexa KW, Gardiner TE, LeRoux M, et al. Structure of a peptidoglycan
619 amidase effector targeted to Gram-negative bacteria by the type VI secretion system. Cell Rep.
620 2012;1:656–64.

621 70. MacIntyre DL, Miyata ST, Kitaoka M, Pukatzki S. The *Vibrio cholerae* type VI secretion system
622 displays antimicrobial properties. Proc Natl Acad Sci USA. 2010;107:19520–4.

623 71. Schwarz S, West TE, Boyer F, Chiang W-C, Carl MA, Hood RD, et al. *Burkholderia* type VI secretion
624 systems have distinct roles in eukaryotic and bacterial cell interactions. PLOS Pathog.
625 2010;6:e1001068.

626 72. Fast D, Kostiuk B, Foley E, Pukatzki S. Commensal pathogen competition impacts host viability. Proc
627 Natl Acad Sci USA. 2018;115:7099–104.

628 73. Logan SL, Thomas J, Yan J, Baker RP, Shields DS, Xavier JB, et al. The *Vibrio cholerae* type VI secretion
629 system can modulate host intestinal mechanics to displace gut bacterial symbionts. Proc Natl Acad Sci
630 USA. 2018;115:3779–87.

631 74. Zhao W, Caro F, Robins W, Mekalanos JJ. Antagonism toward the intestinal microbiota and its effect
632 on *Vibrio cholerae* virulence. Science. 2018;359:210–3.

633

634

Figure legends

Fig. 1. T6SS and VgrG1a and VgrG1b module gene clusters of *Pseudomonas protegens* CHA0 and orthologous genomic regions in *Pseudomonas aeruginosa* PAO1.

Sequence identities and predicted functions are detailed in Supplementary Table S5. PAO1 genes that are absent in the CHA0 genome are shown as empty arrows. Numbers indicate the locus tags for *P. protegens* CHA0 (prefix PFLCHA0_RS…) and *P. aeruginosa* PAO1 (prefix PA…).

Fig. 2. The T6SS and the VgrG modules contribute to insect pathogenicity of *Pseudomonas protegens* CHA0 upon oral infection but not upon injection.

(**a**) Oral activity was tested by feeding larvae of *Pieris brassicae* artificial diet inoculated with 5×10^6 cells of wild type CHA0 or its ΔT6SS, ΔVgrG1a-mod or ΔVgrG1b-mod mutants and monitoring their survival daily during one week. (**b**) Systemic activity was tested by injecting 10^2 cells of the bacterial strains directly into the hemolymph of the larvae and checking their survival hourly, starting at 19 h post-injection. The feeding and injection experiments were repeated six and five times, respectively, with 18 larvae per treatment in each individual experiment. Sterile NaCl solution at 0.9% served as negative control. Data were analyzed using the mixed effect Cox model incorporating the experiment repetition factor and one-way ANOVA followed by Tukey's test with Bonferroni correction. For each panel, treatments with different letters (a, b or c) significantly differed from each other ($P < 0.05$).

Fig. 3. Contribution of the T6SS and the VgrG modules of *Pseudomonas protegens* CHA0 to the colonization of the gut (**a**), the hemolymph (**b**) and the excrements (**c**) of larvae of *Pieris brassicae* following oral infection.

Larvae were fed with a small piece of artificial diet containing 10^7 cells of GFP-tagged variants of wild type CHA0 or its ΔT6SS, ΔVgrG1a-mod or ΔVgrG1b-mod mutants. The T6SS mutant (upper figure panels below insect scheme) and the VgrG module mutants (lower figure panels) were tested in separate

661 experiments. Data show CFU counts of bacterial inoculants per mg of gut, hemolymph or excrements
662 of individual larvae determined at 24 h post oral infection. Each dot corresponds to one insect. Each
663 box-plot graph represents the median of the colonization levels calculated from three independent
664 experiments that were carried out with nine larvae per treatment in each experiment. For the
665 statistical analysis, a Student's t-test was performed to detect significant differences between the
666 colonization levels of the wild type CHA0 and the ΔT6SS mutant. ANOVA followed by Fisher's LSD test
667 was done to detect significant differences between the colonization levels of CHA0 and the VgrG1a
668 and VgrG1b module mutants. *P*-value < 0.001 (***) and *P*-value < 0.05 (*).
669
670 **Fig. 4**. The T6SS contributes to changes induced in the gut microbiome composition of larvae of *Pieris*
671 *brassicae* upon invasion by *Pseudomonas protegens*, impacting in particular on members of the
672 *Enterobacteriaceae* family.
673 (**a**) Gut bacterial composition following oral infection with wild type CHA0 or its ΔT6SS, ΔVgrG1a-mod
674 or ΔVgrG1b-mod mutants. Larvae were fed with a small piece of artificial diet containing 10^7 inoculant
675 cells and were dissected 24 h later to retrieve their guts. Control larvae were fed sterile diet. For each
676 treatment, 10 samples were prepared each containing the pooled guts from four larvae. DNA
677 preparation and 16S rRNA gene-based metagenome sequencing were performed by GenoScreen (Lille,
678 France). The gut bacterial composition was determined using non-transformed abundance data and
679 the eight most abundant families are presented.
680 Box-plots illustrate the effects of wild type CHA0 and the T6SS and VgrG module mutants on the
681 median relative abundance of the *Enterococcaceae* (**b**) and *Enterobacteriaceae* (**c**) families in the insect
682 guts. The data from the abundance matrix were transformed using total sum scaling (TSS) and
683 cumulative sum scaling (CSS) normalization [44] and statistically analyzed using the CALYPSO pipeline
684 [43]. *P*-value < 0.01 (**), *P*-value < 0.05 (*) and *P*-value between 0.05 and 0.09 (.).
685

Fig. 5. The T6SS and the VgrG1a module contribute to interbacterial competition of *Pseudomonas protegens* CHA0 with *Enterobacter* sp. (**a**) but not with *Enterococcus* sp. (**b**) isolated from the gut of *Pieris brassicae* larvae.

Competition of *P. protegens* wild type CHA0, the ΔT6SS mutant or the ΔVgrG1a-mod or ΔVgrG1b-mod mutants against *Enterobacter* sp. and *Enterococcus* sp. was assessed in filter spot assays. CFU quantifications were performed at t = 0 h and t = 24 h based on the antibiotic resistance profiles of the strains as detailed in the Supplementary information. The competitive index (CI) of the competitor was calculated as follows: $CI = [CFU_{competitor\_24\ h}/CFU_{gut\ isolate\_24\ h}] / [CFU_{competitor\_0\ h}/CFU_{gut\ isolate\_0\ h}]$. Boxplots represent data from three independent experiments, each with three replicate strain confrontations. Each dot corresponds to one confrontation. Data were analyzed using an ANOVA followed by HSD of Tukey. Statistical differences between the competitive indices of CHA0 mutants in confrontations with *Enterobacter* are indicated with letters a and b ($P < 0.05$). No statistical differences were found in the competitions with *Enterococcus*.

Fig. 6. Interaction model between *Pseudomonas protegens* and the plant pest insect *Pieris brassicae*.

Step 1: Oral infection; *P. protegens* cells (red) are ingested by the larvae. Step 2: *P. protegens* cells follow the path of food through the gut and establish in this insect compartment. In the gut, the microflora is mainly composed of *Enterococcus* sp. (green cells) and *Enterobacter* sp. (blue cells). Step 3: *P. protegens* cells cross the gut epithelial barrier by a yet unknown mechanism to reach the hemocoel. For this step, the bacteria need to find their way through the indigenous microflora that can aggregate onto the epithelial cells to form an additional protective layer [65, 68]. *P. protegens* uses its T6SS and the associated VgrG1a module, encompassing the VgrG1a spike along with the RhsA effector, to kill *Enterobacter* locally in the vicinity of the gut epithelial cells. Step 4: Once in the hemocoel, *P. protegens* starts to proliferate. Step 5: The bacteria produce virulence factors, among which the entomotoxin Fit [13] that is specifically produced in the hemolymph of the insect [8, 16]. During invasion, a particular LPS decoration protects *P. protegens* against antimicrobial peptides

712 (cecropins) produced by the host [15] and additional virulence factors such as hydrogen cyanide, cyclic
713 lipopeptides, chitinase and phospholipase aid to promote pathogenesis [5, 10, 11]. As soon as the
714 bacteria invade the hemocoel compartment, the insect enters in an acute disease phase leading to its
715 death within about one day. IM, inner membrane; P, periplasm; OM, outer membrane.
716

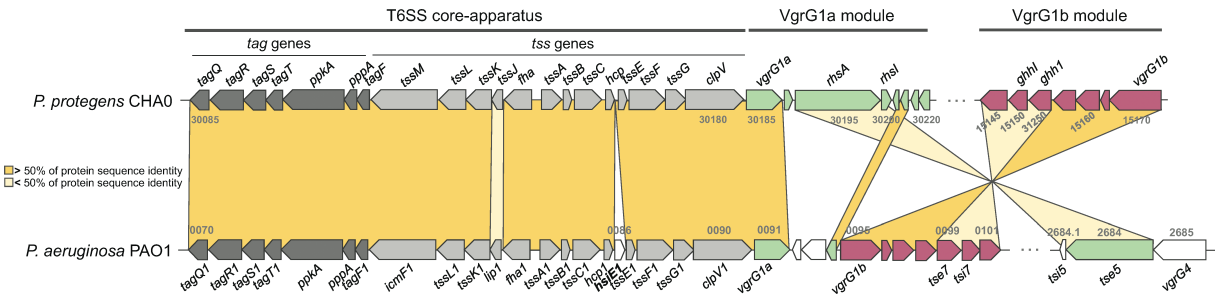
T6SS core-apparatus
VgrG1a module
VgrG1b module
tag genes
tss genes
P. protegens CHA0
P. aeruginosa PAO1
> 50% of protein sequence identity
< 50% of protein sequence identity

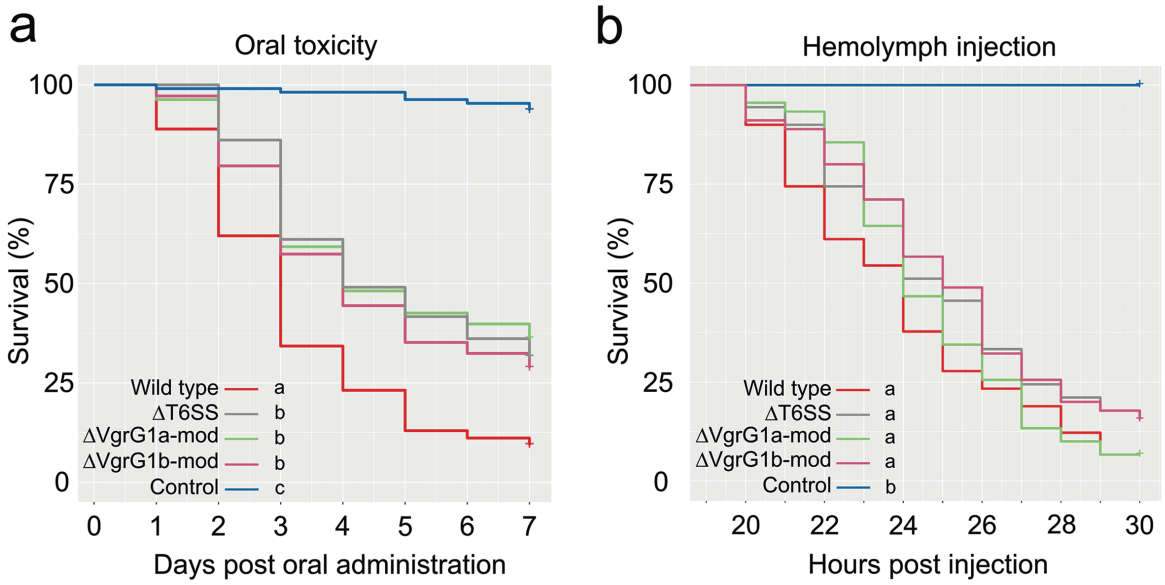
a
Oral toxicity
Survival (%)
Days post oral administration
Wild type a
ΔT6SS b
ΔVgrG1a-mod b
ΔVgrG1b-mod b
Control c
b
Hemolymph injection
Survival (%)
Hours post injection
Wild type a
ΔT6SS a
ΔVgrG1a-mod a
ΔVgrG1b-mod a
Control b

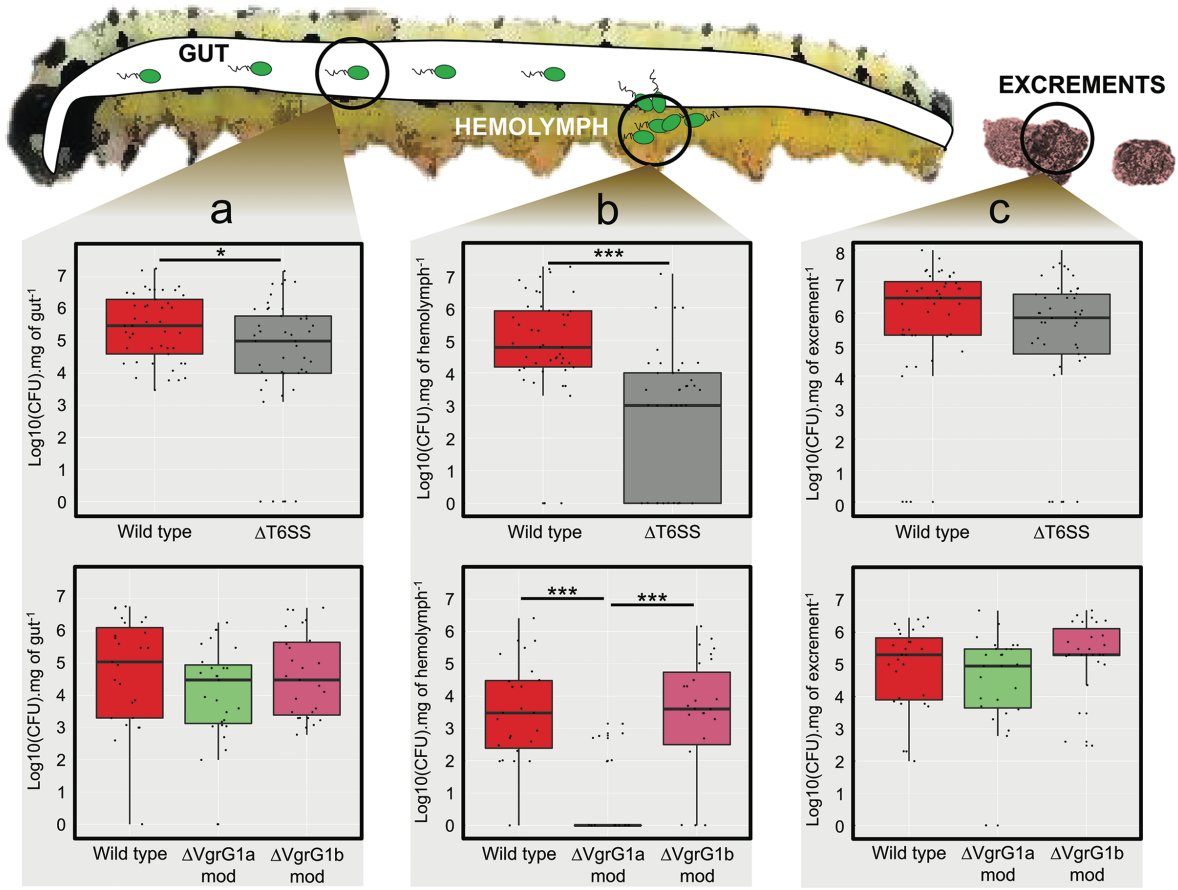
GUT
HEMOLYMPH
EXCREMENTS
a
b
c
Log10(CFU).mg of gut-1
Log10(CFU).mg of hemolymph-1
Log10(CFU).mg of excrement-1
Wild type
ΔT6SS
ΔVgrG1a mod
ΔVgrG1b mod

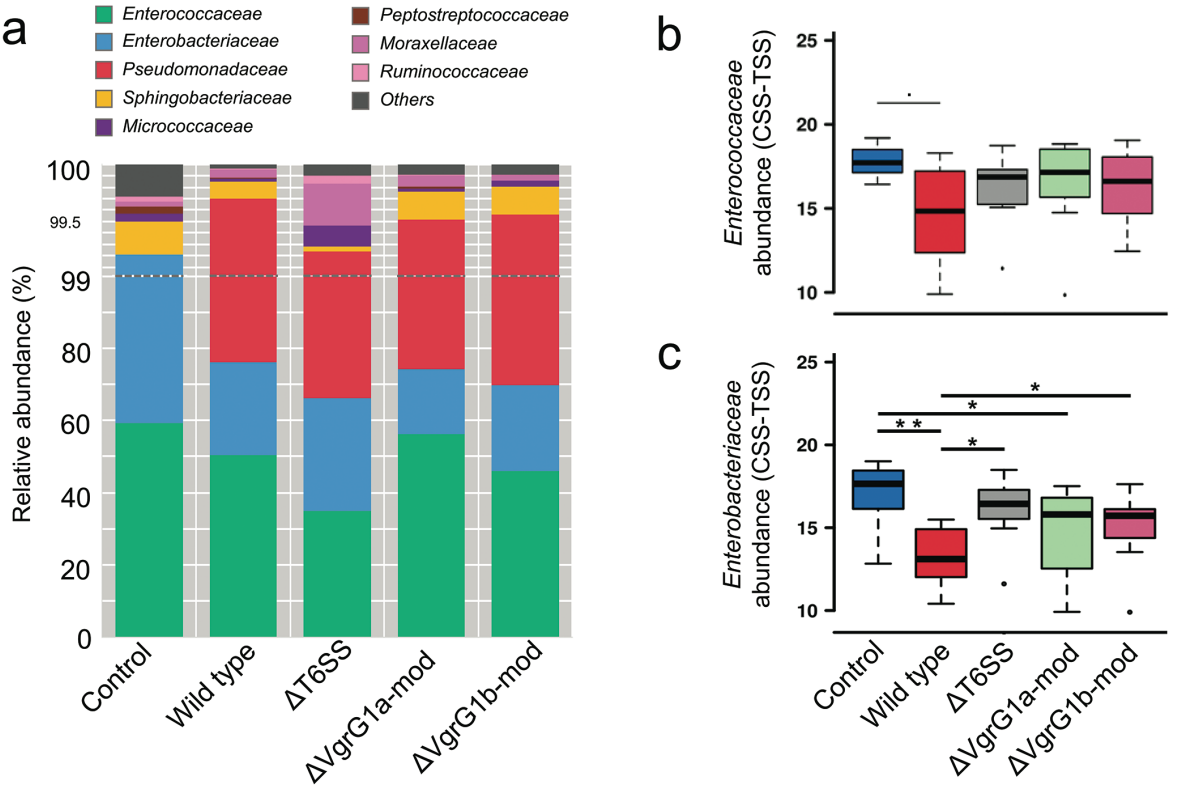
a
Enterococcaceae
Enterobacteriaceae
Pseudomonadaceae
Sphingobacteriaceae
Micrococcaceae
Peptostreptococcaceae
Moraxellaceae
Ruminococcaceae
Others
Relative abundance (%)
Control
Wild type
ΔT6SS
ΔVgrG1a-mod
ΔVgrG1b-mod
b
Enterococcaceae abundance (CSS-TSS)
c
Enterobacteriaceae abundance (CSS-TSS)

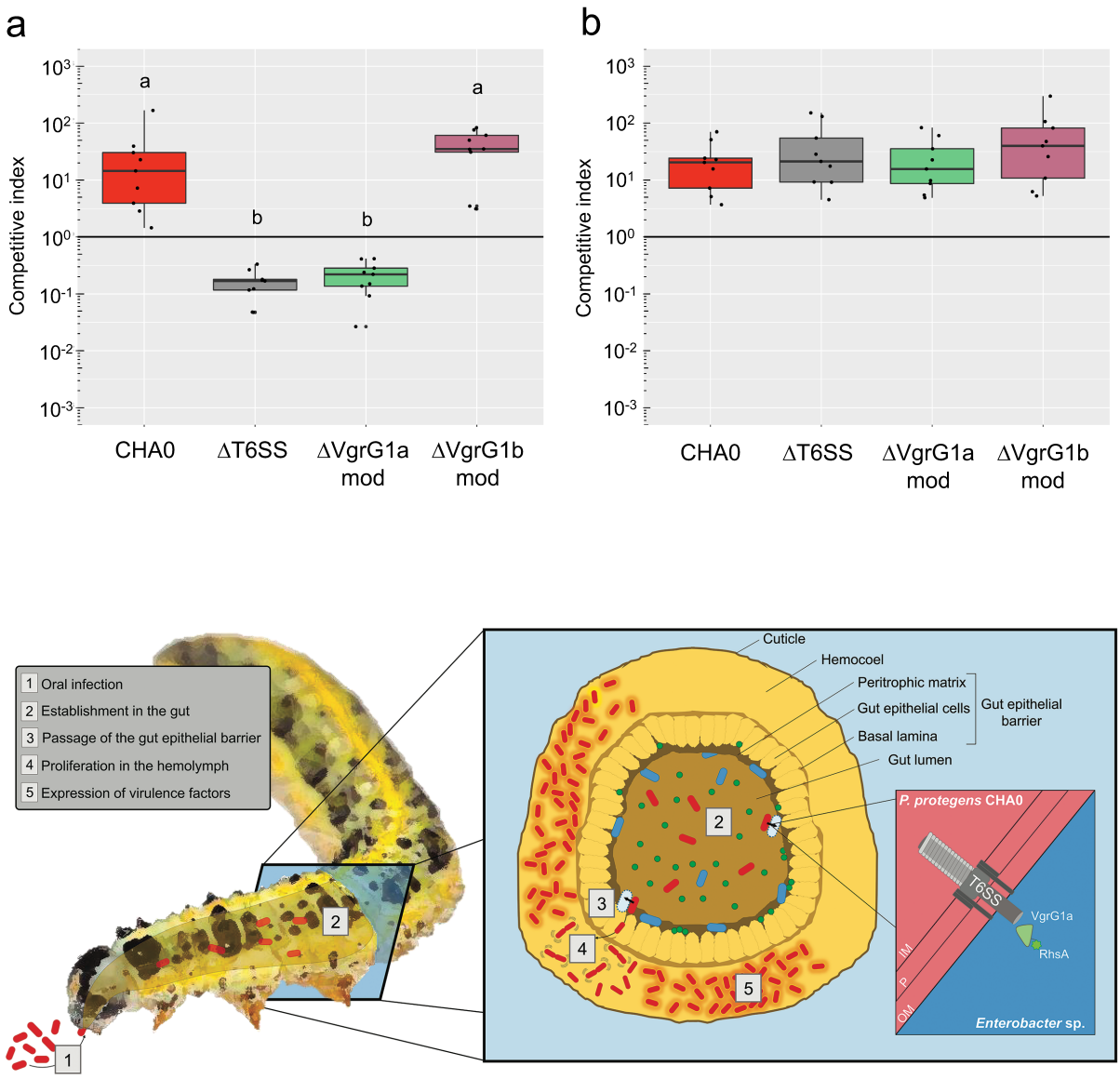
a
b
Competitive index
10^3
10^2
10^1
10^0
10^{-1}
10^{-2}
10^{-3}
a
b
b
a
CHA0
ΔT6SS
ΔVgrG1a mod
ΔVgrG1b mod
1 Oral infection
2 Establishment in the gut
3 Passage of the gut epithelial barrier
4 Proliferation in the hemolymph
5 Expression of virulence factors
Cuticle
Hemocoel
Peritrophic matrix
Gut epithelial cells
Basal lamina
Gut lumen
Gut epithelial barrier
P. protegens CHA0
T6SS
VgrG1a
RhsA
IM
P
OM
Enterobacter sp.

Vacheron *et al*. T6SS contributes to gut microbiome invasion and killing of an herbivorous pest insect by plant-beneficial *Pseudomonas protegens.*

SUPPLEMENTARY INFORMATION

Supplementary Methods

Bacterial strains, culture conditions and *in vitro* competition assays

Bacterial strains and plasmids used in this study are listed in Supplementary Tables 1 and 2. Bacteria were routinely cultured on nutrient agar (NA), in nutrient yeast broth (NYB) or in lysogeny broth (LB) [1]. When required, growth media were supplemented with ampicillin (100 µg ml^{-1}), chloramphenicol (50 µg ml^{-1}), gentamycin (10 µg ml^{-1}) or kanamycin (25 µg ml^{-1}). The incubation temperatures were 25°C for *Pseudomonas* strains and insect gut isolates and 37°C for *Escherichia coli* if not otherwise specified. Electro-competent cells of *P. protegens* were obtained at 35°C.

16S rRNA gene sequencing for metagenomic analysis

DNAs were extracted from *Pieris* gut content using a protocol developed and standardized by GenoScreen (Lille, France) based on the QIAamp Fast DNA Stool Mini kit (Qiagen, USA). DNAs were then quantified by fluorescence. The amplicon library was generated by targeting the V3 and V4 hypervariable regions of the 16S rDNA with 5 ng of extracted DNA per sample using 192 bar-coded primers (Metabiote MiSeq Primers). The final library was obtained by equimolary pooling amplicons. Illumina MiSeq sequencing (2 x 250 nt) was performed. Sequence data were processed using the GenoScreen analysis pipeline MetaBiote® OnLine. Sequences were denoised, OTUs generated and chimeras removed. Operational taxonomic units (OTUs) were defined by clustering at 3% divergence (97% similarity). Final OTUs were taxonomically classified by the RDP method using the Greengenes database. The 16S-metagenomic data were deposited at the European Nucleotide Archive as BioProject ID PRJEB28754, samples ERS2756952 to ERS2757001.

Isolation of bacteria from the gut microbiota of *P. brassicae* larvae

To isolate *Enterobacter* sp. and *Enterococcus* sp., the guts of surface-disinfested 3rd instar larvae were extracted and pooled by three in Eppendorf tubes containing 1 ml of sterile 0.9% NaCl solution and glass beads. The tubes were agitated using a FastPrep-24™ 5G homogenizer, for 1 min at 6 $m.s^{-1}$. The obtained homogenate was diluted and plated on NA plates that were incubated overnight at room temperature. Colonies were purified by subculturing and isolates with similar or different phenotypic characteristics were subjected to colony PCR using universal primers UV-F and UV-R (Supplementary Table 3) targeting a part of the bacterial 16S rRNA gene [2]. The amplicons were purified with the QIAquick® PCR Purification Kit (Qiagen®) and sent for sequencing (GATC Biotech). Sequences were subjected to BLAST® analysis in order to identify the isolated bacteria.

Interbacterial competition assays

Killing activities of *P. protegens* wild type CHA0, the ΔT6SS mutant or the ΔVgrG1a-mod or ΔVgrG1b-mod mutants against *Enterobacter* sp. or *Enterococcus* sp. isolated from the insect gut (see above) were tested in confrontation assays on filters as follows. Over-night cultures were washed with 0.9% NaCl and their OD_{600nm} was adjusted to 0.1. Aliquots of 50 µl of the adjusted cultures were mixed at a ratio of 1:1 and spotted onto a sterile 0.2-µm cellulose acetate membrane filter (Sartorius) with a diameter of 25 mm placed on a NA plate. Following incubation at 25°C for 24 h, the bacterial growth on each filter was suspended in 5 ml of sterile 0.9% NaCl solution. The resulting cell suspensions were serially diluted and aliquots of 10 µl were spotted onto the appropriate NA plates with or without antibiotic depending on the specific confrontation as follows. In the *Enterococcus* vs. *Pseudomonas* competition assays, *Enterococcus* sp. were selected on NA with 10 µg ml^{-1} of gentamycin and *Pseudomonas* strains on NA with 200 µg ml^{-1} of ampicillin, with incubation at 25°C. In the *Enterobacter* vs. *Pseudomonas* sp. competition assay, *Enterobacter* sp. were selected on NA without antibiotic and incubation at 42°C, and *Pseudomonas* strains on NA with 25 µg ml^{-1} of spectinomycin with incubation at 25°C. The CFU counts of the competitors (CHA0 WT or derivatives) and the gut isolates were determined at t = 0 h and t = 24 h and used to calculate the competitive index (CI) as follows: $CI = [CFU_{competitor\text{-}24\ h}/CFU_{gut\ isolate\text{-}24\ h}] / [CFU_{competitor\text{-}0\ h}/CFU_{gut\ isolate\text{-}0\ h}]$.

Supplementary Figures

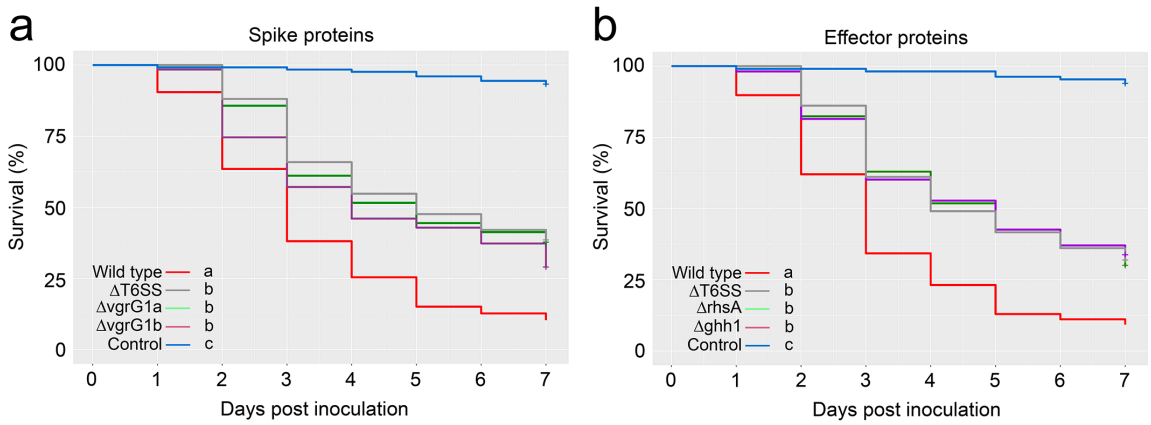

Fig. S1. The VgrG spikes and the effectors encoded by the VgrG1a and VgrG1b modules contribute to the insect pathogenicity of *Pseudomonas protegens* CHA0 following oral infection.
The virulence of the CHA0 mutants lacking the VgrG1a or VgrG1b spikes (**a**) or the effectors RhsA or times. Results were pooled and analyzed using the mixed effect Cox model and one-way ANOVA followed by Tukey's test with Bonferroni correction. For each panel, treatments with different letters (a, b or c) significantly differed from each other ($P < 0.05$).

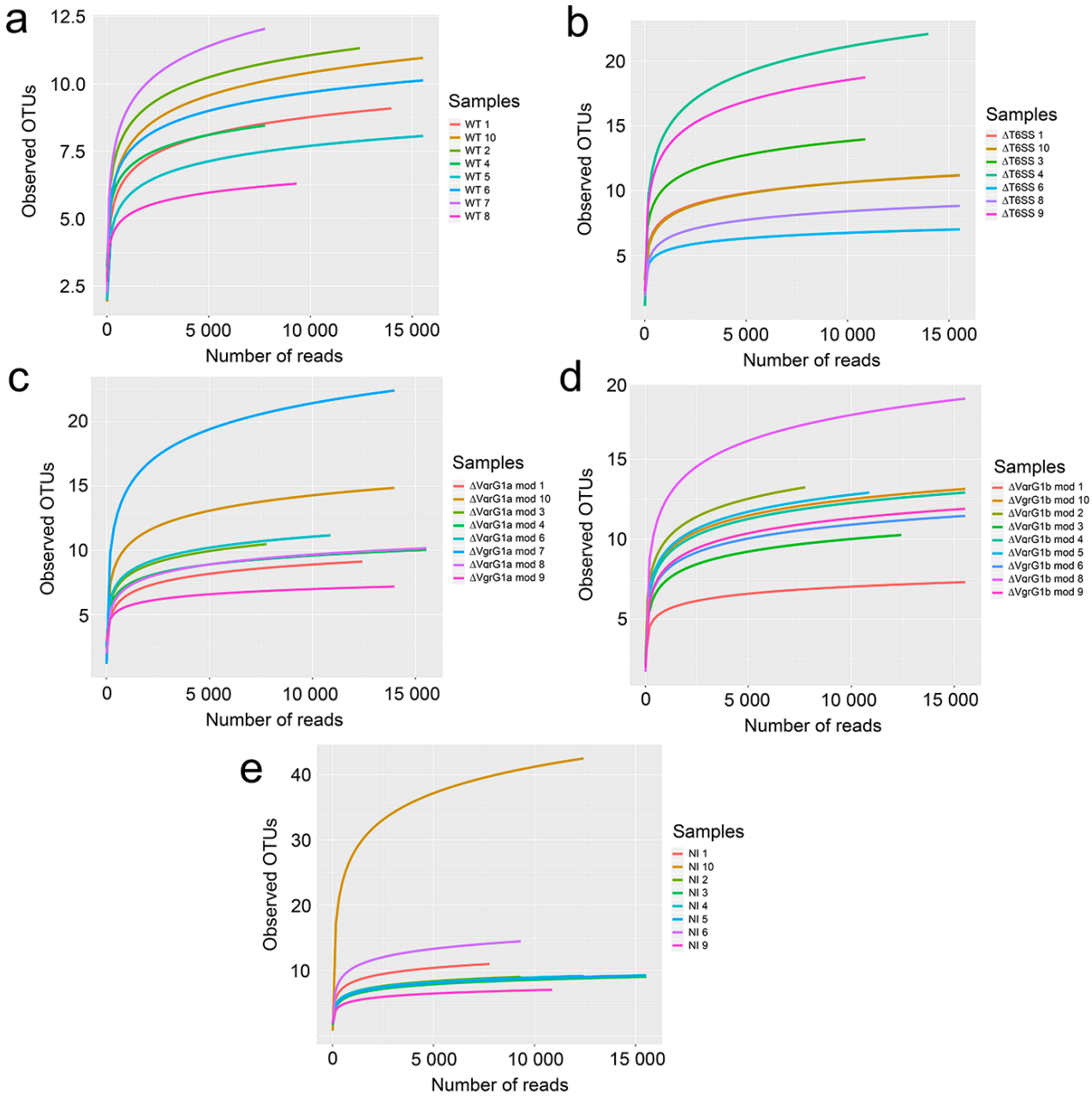

Fig. S2. Rarefaction curves of OTUs for the bacterial community samples.
The plot shows the number of OTUs as a function of the number of reads sampled. The rarefaction curves were made for each tested condition, i.e. (**a**) WT, *P. protegens* CHA0 wild type; (**b**) ΔT6SS mutant of CHA0; (**c**) ΔVgrG1a-mod mutant of CHA0; (**d**) ΔVgrG1b-mod mutant of CHA0; and (**e**) NI, non-inoculated control.

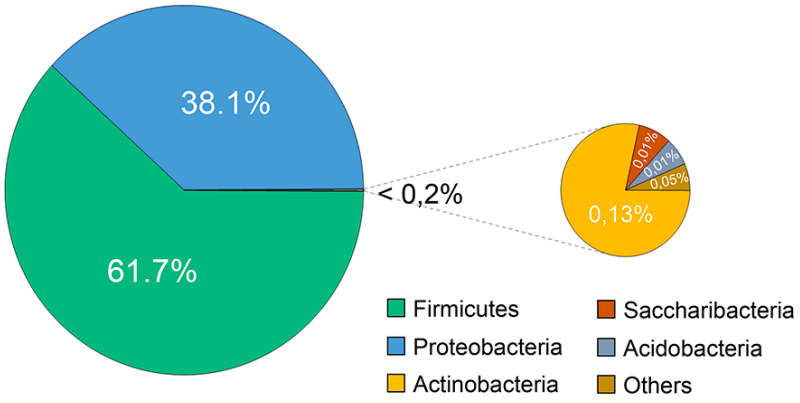

Fig. S3. Bacterial community composition at phylum level in the gut of *Pieris brassicae* larvae.
The percentage values indicate the relative abundance of each phylum. DNAs were obtained from eight insect gut samples. Each sample was prepared from the pooled entire guts of four larvae. Preparation and metagenomic analysis of 16S rRNA gene amplicon libraries was performed by GenoScreen (Lille, France) using the Metabiote® pipeline.

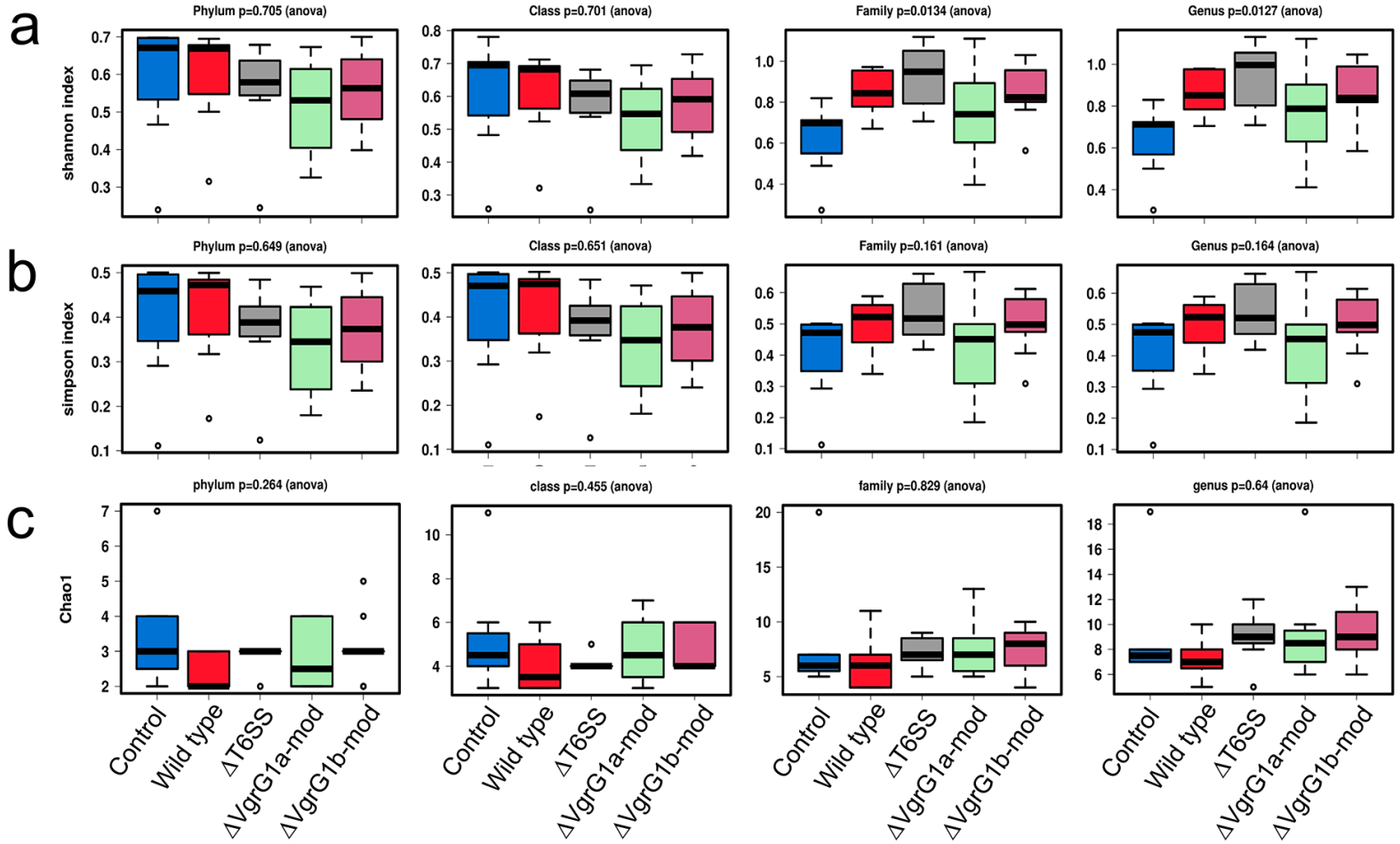

Fig. S4. Comparison of bacterial diversity between conditions using different α-diversity indexes.
The calculation of the Shannon-Weaver (**a**), Simpson (**b**) and Chao1 (**c**) α-diversity indexes was done at different taxa levels, i.e. phylum, class, family and genus. Data are expressed as standard boxplots with medians. Differences of bacterial diversity among the different conditions (non-inoculated control, inoculation with *Pseudomonas protegens* CHA0 wild type or the ΔT6SS, ΔVgrG1a-mod or ΔVgrG1b-mod mutants) were determined using ANOVA coupled with Tukey's HSD ($P < 0.05$).

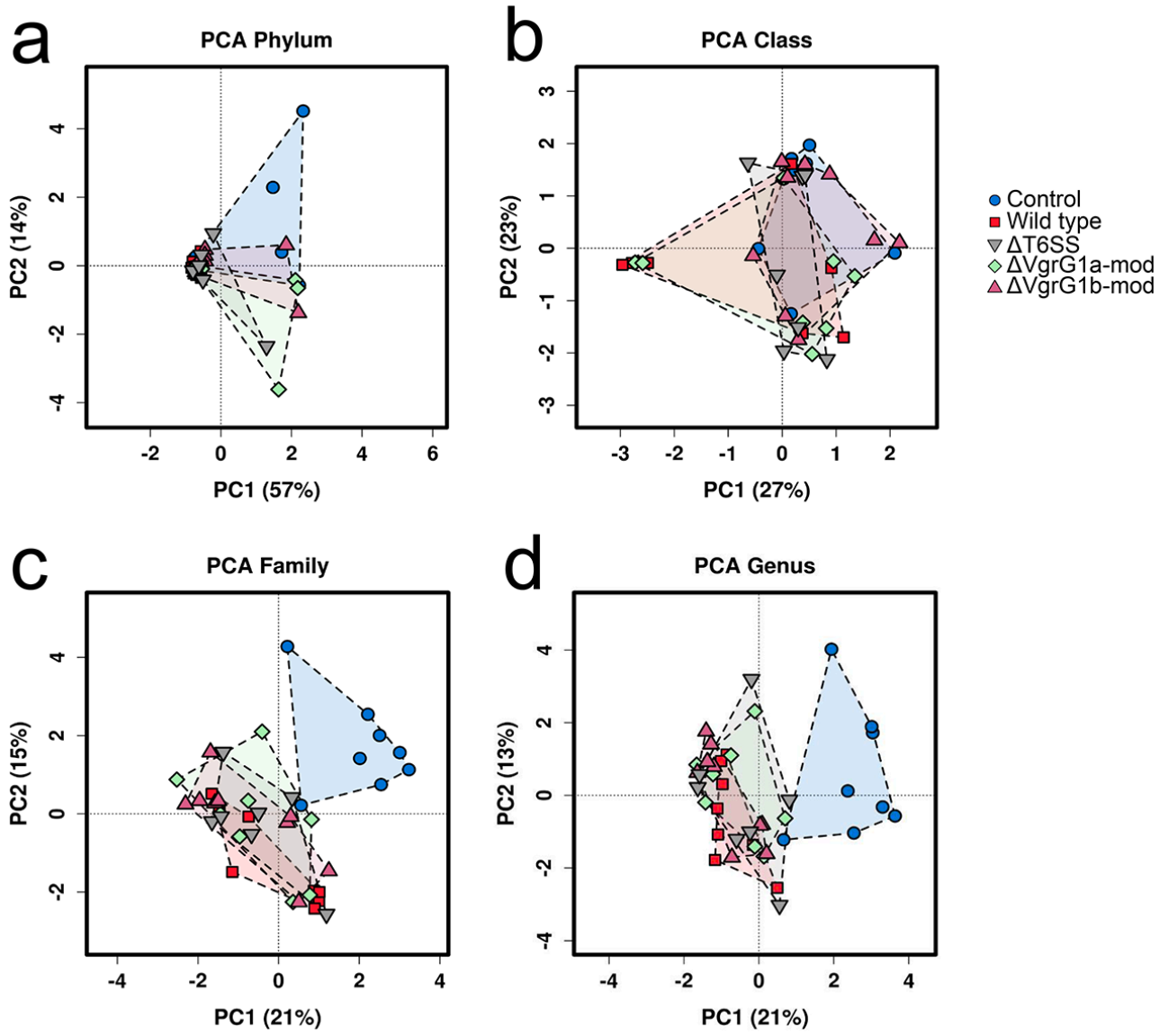

Fig. S5. Principal Component Analysis (PCA) of the β-diversity.
The β-diversity for the different conditions, i.e. non-inoculated control and inoculation with *P. protegens* CHA0 wild type or the ΔT6SS, ΔVgrG1a-mod or ΔVgrG1b-mod mutants, was assessed at different taxa levels, i.e. (**a**) phylum, (**b**) class, (**c**) family and (**d**) genus. Each point corresponds to a sample. Four insect guts were pooled per sample.

Supplementary Tables

Table S1. Bacterial strains used in this study.

Strain name	Strain code	Genotype or relevant characteristics[1]	Reference or source
Pseudomonas protegens			
CHA0	CHA0	Wild type, genome accession number NC_021237.1	[3, 4]
CHA0-*gfp2*	CHA0-*gfp2*	CHA0::attTn*7*-*gfp2*; Gm^r	[5]
ΔT6SS	CHA5175	Δ*T6SS* mutant of CHA0; deletion of PFLCHA0_RS30085 through PFLCHA0_RS30180	This study
ΔT6SS-*gfp2*	CHA5175-*gfp2*	Δ*T6SS*::attTn*7*-*gfp2*; Gm^r	This study
ΔVgrG1a-mod	CHA5200	Δ*vgrG1a-mod* mutant of CHA0; deletion of the VgrG1a module encompassing PFLCHA0_RS30185 through PFLCHA0_RS30200	This study
ΔVgrG1a-mod-*gfp2*	CHA5200-*gfp2*	Δ*vgrG1a-mod*::attTn*7*-*gfp2*; Gm^r	This study
ΔVgrG1b-mod	CHA5086	Δ*vgrG1b-mod* mutant of CHA0; deletion of the VgrG1b module encompassing PFLCHA0_RS15145 through PFLCHA0_RS15190	This study
ΔVgrG1b-mod-*gfp2*	CHA5086-*gfp2*	Δ*vgrG1b-mod*::attTn*7*-*gfp2*; Gm^r	This study
ΔvgrG1a	CHA5215	Δ*vgrG1a* mutant of CHA0; deletion of VgrG1a module spike gene	This study
ΔvgrG1b	CHA5112	Δ*vgrG1b* mutant of CHA0; deletion of VgrG1b module spike gene	This study
ΔrhsA	CHA5257	Δ*rhsA* deletion mutant of CHA0; deletion of the VgrG1a module effector gene	This study
Δghh1	CHA5209	Δ*ghh1* mutant of CHA0; deletion of the VgrG1b module effector gene	This study
Insect gut isolates			
Enterobacter sp.		Isolated from the gut of *Pieris brassicae*	This study
Enterococcus sp.		Isolated from the gut of *Pieris brassicae*	This study
Escherichia coli			
S17-1/λpir		Laboratory strain	[6]
DH5α		Laboratory strain	[1]

[1] Gm^r, gentamycin resistance.

Table S2. Plasmids used in this study.

Plasmids	Genotype or relevant characteristics[1]	Reference or source
pBK-miniTn7-*gfp2*	pUC19-based delivery plasmid for miniTn*7*-*gfp*2; mob$^+$; Gm^r, Cm^r, Ap^r	[7]
pEMG	pSEVA212S; oriR6K, *lacZα* with two flanking I-SceI sites; Km^r, Ap^r	[8]
pME8306	pEMG::Δ*vgrG1b mod* suicide plasmid for the deletion of the VgrG1b module, i.e. PFLCHA0_RS15145 through PFLCHA0_RS15190 encompassing the *vgrG1b*, *ghh1* and *ghhI* genes	This study
pME8329	pEMG::Δ*vgrG1b*; suicide plasmid for the in-frame deletion of the VgrG1b spike gene (PFLCHA0_RS15170)	This study
pME8384	pEMG::Δ*T6SS* suicide plasmid for the deletion of the T6SS core apparatus genes encompassing PFLCHA0_RS30085 through PFLCHA0_RS30180	This study
pME9407	Carrier plasmid for mini-Tn*7*-*mcherry*; Gm^r, Ap^r	[9]
pME11025	pEMG::Δ*ghh1*; suicide plasmid for the in-frame deletion of the VgrG1b module effector gene *ghh1* (PFLCHA0_RS31250)	This study
pME11035	pEMG::Δ*vgrG1a*; suicide plasmid for the in-frame deletion of the VgrG1a spike gene (PFLCHA0_RS30185)	This study
pME11055	pEMG::Δ*rhsA*; suicide plasmid for the in-frame deletion of the VgrG1a module effector gene *rhsA* (PFLCHA0_RS30195)	This study
pME11056	pEMG::Δ*vgrG1a-mod* suicide plasmid for the deletion of the VgrG1a module, i.e. PFLCHA0_RS30185 through PFLCHA0_RS30200 encompassing the *vgrG1a*, *rhsA* and *rhsI* genes	This study
pSW-2	*ori*RK2, *xylS*, P_m::*I-sce*I; Gm^R	[8]
pUX-BF13	Helper plasmid encoding Tn*7* transposition functions; R6K-replicon; Ap^R	[10]

[1] Ap^r, ampicillin resistance; Cm^r, chloramphenicol resistance; Gm^r, gentamicin resistance; Km^r, kanamycin resistance.

Table S3. Oligonucleotides used in this study.

Oligonucleotide	Sequence 5' → 3', restriction enzyme[1]	Usage
T6SS-1	CGAGCTCCAGGTACTTGGTCAGCCCCT, SacI	Deletion of the T6SS core-apparatus gene cluster (PFLCHA0_RS30085 through RS30180)
T6SS-2	GGGGTACCAGAGCAACAAGGTCGCGACC, KpnI	Deletion of the T6SS core-apparatus gene cluster (PFLCHA0_RS30085 through RS30180)
T6SS-3	GGGGTACCAACTGCACTACGACTTCAGC, KpnI	Deletion of the T6SS core-apparatus gene cluster (PFLCHA0_RS30085 through RS30180)
T6SS-4	CGGGATCCGACGAAATCGAAGCTGGTCT, BamHI	Deletion of the T6SS core-apparatus gene cluster (PFLCHA0_RS30085 through RS30180)
VgrG1a-mod-1	CGAGCTCAAGAACACCCTGATCCTGCT, SacI	Deletion of VgrG1a module gene cluster (PFLCHA0_RS30185 through RS30200)
VgrG1a-mod-2	GGGGTACCCAGTCGTGTGGATTGCTGAA, KpnI	Deletion of VgrG1a module gene cluster (PFLCHA0_RS30185 through RS30200)
VgrG1a-mod-3	GGGGTACCACGATCGCGCATCCTAGCCA, KpnI	Deletion of VgrG1a module gene cluster (PFLCHA0_RS30185 through RS30200)
VgrG1a-mod-4	CGGGATCCACTCTCAAGCGCGTGCCATC, BamHI	Deletion of VgrG1a module gene cluster (PFLCHA0_RS30185 through RS30200)
VgrG1b-mod-1	CGGAATTCATCGACAGGGTATCGAGCAGGG, EcoRI	Deletion of VgrG1b module gene cluster (PFLCHA0_RS15145 through RS15190)
VgrG1b-mod-2	GGGGTACCTTGTTGTCCGGAGGATGAGCAG, KpnI	Deletion of VgrG1b module gene cluster (PFLCHA0_RS15145 through RS15190)
VgrG1b-mod-3	GGGGTACCCAACCAACTTGAAAGTCACGGC, KpnI	Deletion of VgrG1b module gene cluster (PFLCHA0_RS15145 through RS15190)
VgrG1b-mod-4	CGGGATCCGGTGCTTTAAGCGACCATACCT, BamHI	Deletion of VgrG1b module gene cluster (PFLCHA0_RS15145 through RS15190)
vgrG1a-3	GGGGTACCAAAGGCTAATGAACGGACGCC, KpnI	Deletion of *vgrG1a* (PFLCHA0_RS30185)
vgrG1a-4	CGGGATCCATCATCGAGGTGTGTTCCAGC, BamHI	Deletion of *vgrG1a* (PFLCHA0_RS30185)
vgrG1b-1	CGGAATTCAGATTAAACGTGCCTTTGGCCA, EcoRI	Deletion of *vgrG1b* (PFLCHA0_RS15170)
vgrG1b-2	GGGGTACCAACTAGGAGTAACGCGTATGAC, KpnI	Deletion of *vgrG1b* (PFLCHA0_RS15170)
vgrG1b-3	GGGGTACCTGCCATAAACGACTTCCTCTGG, KpnI	Deletion of *vgrG1b* (PFLCHA0_RS15170)
vgrG1b-4	CGGGATCCGTTTTATTCTTTGGCTGCGCGC, BamHI	Deletion of *vgrG1b* (PFLCHA0_RS15170)
rhsA-1	CGGAATTCAAAGGCTAATGAACGGACGC, EcoRI	Deletion of *rhsA* (PFLCHA0_RS30195)
rhsA-2	CCCAAGCTTGAGAATGTCGGCCATCATCG, HindIII	Deletion of *rhsA* (PFLCHA0_RS30195)
rhsA-3	CCCAAGCTTACCTTCTGGCTTCTTCGCTA, HindIII	Deletion of *rhsA* (PFLCHA0_RS30195)
rhsA-4	CGGGATCCGTTCAGTGCTGCCAGTAGTT, BamHI	Deletion of *rhsA* (PFLCHA0_RS30195)
ghh1-1	CGGAATTCCCATCAGAGGCGCATATCAATG, EcoRI	Deletion of *ghh1* (PFLCHA0_RS31250)
ghh1-2	GGGGTACCTGAGCCACCACCCAATAAACGG, KpnI	Deletion of *ghh1* (PFLCHA0_RS31250)
ghh1-3	GGGGTACCCATATTGTTGGCATACACCTCG, KpnI	Deletion of *ghh1* (PFLCHA0_RS31250)
ghh1-4	TCCCCCGGGGCCAGAACTCCAACGGATTTAT, SmaI	Deletion of *ghh1* (PFLCHA0_RS31250)
UV-F[2]	AGRGTTYGATYMTGGCTCAG	Identification of gut-isolated bacteria
UV-R[2]	CCGTCAATTCMTTTRAGTTT	Identification of gut-isolated bacteria

[1] Restriction sites are underlined.
[2] Reference: [2].

Table S4. Filtering process before 16S metagenomic analysis.

Condition	Total number of samples	Number of samples removed from the analysis		Number of samples analyzed
		Low number of reads[1]	Non-infected by *Pseudomonas*[2]	
Control	10	2	NA	8
CHA0 wild type	10	0	2	8
ΔT6SS	10	2	1	7
ΔVgrG1a mod	10	0	2	8
ΔVgrG1b mod	10	0	1	9

[1] Less than 3000 reads.
[2] No *Pseudomonas* OTUs indicative of infection by *P. protegens* inoculants were detected. NA, not applicable.

Table S5. T6SS and VgrG modules genes in *Pseudomonas protegens* CHA0 and orthologs in *Pseudomonas aeruginosa* PAO1.

Gene name	*P. protegens* CHA0 gene accession number [1]	*P. protegens* CHA0 protein accession number	Function	Gene ortholog in *P. aeruginosa* PAO1 [2]	Coverage (%)	Protein identity (%)
Type VI secretion system core apparatus						
tagQ	PFLCHA0_RS30085	WP_011064242.1	Hypothetical protein	*tagQ1* (PA0070)	95	55
tagR	PFLCHA0_RS30090	WP_015637477.1	Hypothetical protein	*tagR1* (PA0071)	98	78
tagS	PFLCHA0_RS30095	WP_015637478.1	ABC transporter permease	*tagS1* (PA0072)	100	63
tagT	PFLCHA0_RS30100	WP_011064245.1	ABC transporter ATP-binding protein	*tagT1* (PA0073)	99	65
ppkA	PFLCHA0_RS30105	WP_015637479.1	Serine/threonine protein kinase	*ppkA* (PA0074)	100	71
pppA	PFLCHA0_RS30110	WP_011064247.1	Serine/threonine-protein phosphatase	*pppA* (PA0075)	95	74
tagF	PFLCHA0_RS30115	WP_011064248.1	T6SS-associated protein TagF	*tagF1* (PA0076)	98	61
tssM	PFLCHA0_RS30120	WP_015637480.1	T6SS membrane complex subunit TssM	*icmF1* (PA0077)	94	78
tssL	PFLCHA0_RS30125	WP_015637481.1	T6SS membrane complex subunit TssL	*tssL1* (PA0078)	100	76
tssK	PFLCHA0_RS30130	WP_011064251.1	T6SS membrane subunit TssK	*tssK1* (PA0079)	100	77
tssJ	PFLCHA0_RS30135	WP_011064252.1	T6SS membrane complex subunit TssJ	*lip1* or *tssJ1* (PA0080)	97	39
fha	PFLCHA0_RS30140	WP_011064253.1	T6SS-associated FHA domain protein TagH	*fha1* (PA0081)	100	61
tssA	PFLCHA0_RS30145	WP_041752688.1	T6SS protein TssA	*tssA1* (PA0082)	100	59
tssB	PFLCHA0_RS30150	WP_011064255.1	T6SS contractile sheath small subunit	*tssB1* (PA0083)	97	93
tssC	PFLCHA0_RS30155	WP_011064256.1	T6SS contractile sheath large subunit	*tssC1* (PA0084)	100	92
hcp	PFLCHA0_RS30160	WP_011064257.1	T6SS tube protein Hcp	*hcp1* (PA0085)	99	76
tssE	PFLCHA0_RS30165	WP_011064258.1	T6SS baseplate subunit TssE	*tssE1* (PA0087)	98	68
tssF	PFLCHA0_RS30170	WP_011064259.1	T6SS baseplate subunit TssF	*tssF1* (PA0088)	100	81
tssG	PFLCHA0_RS30175	WP_011064260.1	T6SS baseplate subunit TssG	*tssG1* (PA0089)	99	71
clpV	PFLCHA0_RS30180	WP_015637485.1	T6SS ATPase TssH	*clpV1* (PA0090)	99	87
VgrG1a module						
vgrG1a	PFLCHA0_RS30185	WP_011064262.1	T6SS tip protein VgrG	*vgrG1a* (PA0091)	99	71
	PFLCHA0_RS30190	WP_011064263.1	DUF1795 domain-containing protein	No ortholog found	-	-
rhsA	PFLCHA0_RS30195	WP_015637486.1	Protein RhsA	*tse5* (PA2684)	74	29
rhsI	PFLCHA0_RS30200	WP_015637487.1	Hypothetical protein	No ortholog found	-	-

	PFLCHA0_RS30205	WP_015637488.1	Hypothetical protein	No ortholog found	-	-
	PFLCHA0_RS30210	WP_015637489.1	DUF1795 domain-containing protein	*EagT6* (PA0094)	100	77
	PFLCHA0_RS30215	WP_015637490.1	Putative lipoprotein	No ortholog found	-	-
	PFLCHA0_RS30220	WP_041752690.1	Hypothetical protein	No ortholog found	-	-
VgrG1b module						
	PFLCHA0_RS15145	WP_015635603.1	Conserved hypothetical protein	PA0101	98	63
ghhI	PFLCHA0_RS15150	WP_041752250.1	Hypothetical protein	*tsi7* (PA0100)	95	35
ghh1	PFLCHA0_RS31250	WP_015635604.1	DUF4150, Tox-GHH2, and PAAR domains containing protein	*tse7* (PA0099)	91	48
	PFLCHA0_RS15155	WP_015635605.2	3-Oxoacyl-ACP synthase	PA0098	99	74
	PFLCHA0_RS15160	WP_015635606.0	DUF2169 domain-containing protein	PA0097	100	65
	PFLCHA0_RS15165	WP_015635607.1	Hypothetical protein with a portion of VgrG domain	PA0096	100	61
vgrG1b	PFLCHA0_RS15170	WP_015635608.1	T6SS tip protein VgrG	*vgrG1b* (PA0095)	100	73

[1] Genome accession number of *P. protegens* CHA0: NC_021237.1.

[2] Genome accession number of *P. aeruginosa* PAO1: NC_002516.2.

Table S6. Relative abundance of OTUs affiliated to the *Enterococcaceae* and *Enterobacteriaceae* families in the gut microbiomes of *Pieris brassicae* larvae following oral infection by *Pseudomonas protegens* CHA0 wild type or its T6SS or VgrG module mutants.

#OTU ID	Genus affiliation	Relative abundance (%) inside the family per condition[1]				
		Non-inoculated	Wild type CHA0	ΔT6SS	ΔVgrG1a-mod	ΔVgrG1b-mod
Enterococcaceae						
denovo2983	*Enterococcus*	99.98	99.98	99.99	99.98	99.96
denovo2721	*Enterococcus*	>0.10	>0.10	>0.10	>0.10	>0.10
denovo2379	*Enterococcus*	-	-	-	-	>0.10
denovo588	*Enterococcus*	>0.10	-	-	-	>0.10
Enterobacteriaceae						
denovo3889	*Enterobacter*	98.26	98.69	98.90	96.16	97.69
denovo966	*Escherichia*	1.21	0.93	0.41	2.07	1.86
denovo3152	*Enterobacter*	0.50	0.30	0.52	0.35	0.43
denovo3677	No genus affiliated	-	>0.10	>0.10	1.39	>0.10
denovo3436	*Citrobacter*	-	-	>0.10	>0.10	-
denovo4425	*Enterobacter*	>0.10	>0.10	-	-	-
denovo3577	*Shigella*	>0.10	-	-	-	-
denovo4046	No genus affiliated	-	-	>0.10	-	-
denovo2632	No genus affiliated	-	-	>0.10	-	-
denovo906	*Salmonella*	>0.10	-	-	-	-
denovo943	*Enterobacter*	-	>0.10	-	-	-
denovo951	*Citrobacter*	>0.10	-	-	-	-

[1] -, not detected.

References

1. Sambrook J, Fritsch EF, Maniatis T. Molecular cloning: a laboratory manual. Molecular cloning: a laboratory manual 1989..
2. Rigsbee L, Agans R, Foy B. Optimizing the analysis of human intestinal microbiota with phylogenetic microarray. FEMS Microbiol Ecol. 2011;75:332-42.
3. Stutz EW, Défago G, Kern H. Naturally occurring fluorescent pseudomonads involved in suppression of black root rot of tobacco. Phytopathology. 1986;76:181–5
4. Jousset A, Schuldes J, Keel C, Maurhofer M, Daniel R, Scheu S, et al. Full-genome sequence of the plant growth-promoting bacterium *Pseudomonas protegens* CHA0. Genome Announc. 2014; 2:e00322–14.
5. Péchy-Tarr M, Borel N, Kupferschmied P, Turner V, Binggeli O, Radovanovic D, et al. Control and host-dependent activation of insect toxin expression in a root-associated biocontrol pseudomonad. Environ Microbiol. 2013;15:736-50.
6. Simon R, Priefer U, Pühler A. A broad host range mobilization system for in vivo genetic engineering: transposon mutagenesis in Gram negative bacteria. Nat Biotechnol. 1983;1:784–91.
7. Koch B, Jensen LE, Nybroe O. A panel of Tn*7*-based vectors for insertion of the *gfp* marker gene or for delivery of cloned DNA into Gram-negative bacteria at a neutral chromosomal site. J Microbiol Meth. 2001;45:187–95.
8. Martínez-García E, de Lorenzo V. Engineering multiple genomic deletions in Gram-negative bacteria: analysis of the multi-resistant antibiotic profile of *Pseudomonas putida* KT2440. Environ Microbiol. 2011;13:2702–16.
9. Rochat L, Péchy-Tarr M, Baehler E, Maurhofer M, Keel C. Combination of fluorescent reporters for simultaneous monitoring of root colonization and antifungal gene expression by a biocontrol pseudomonad on cereals with flow cytometry. Mol Plant Microbe Interact. 2010;23:949–61.
10. Bao Y, Lies DP, Fu H, Roberts GP. An improved Tn*7*-based system for the single-copy insertion of cloned genes into chromosomes of gram-negative bacteria. Gene. 1991;109:167–8.